A REVISED DESIGN CONCEPT FOR THE A-7E APPROACH POWER COMPENSATOR SYSTEM

David Haley Finney

Library
Naval Postgraduate School
Monterey, California 93940

NAVAL POSTGRADUATE SCHOOL
Monterey, California

THESIS

A REVISED DESIGN CONCEPT

FOR

THE A-7E APPROACH POWER COMPENSATOR SYSTEM

by

DAVID HALEY FINNEY

Thesis Advisor: Ronald A. Hess

March 1973

T253784

Approved for public release; distribution unlimited.

A Revised Design Concept
for
the A-7E Approach Power Compensator System

by

David Haley Finney
Lieutenant, United States Navy
B.S., United States Naval Academy, 1967

Submitted in partial fulfillment of the
requirements for the degree of

MASTER OF SCIENCE IN AERONAUTICAL ENGINEERING

from the

NAVAL POSTGRADUATE SCHOOL
March 1973

Library
Naval Postgraduate School
Monterey, California 93940

ABSTRACT

The present concept of automatic throttle control, as employed in Navy carrier-based aircraft, was investigated. The aircraft chosen for study was the A-7E. The powerplant was the TF41-A-2, a turbofan engine with a relatively slow throttle response in the approach power range.

The effects of additional inputs to the approach power compensator were evaluated. It was shown that a considerable increase in performance could be achieved through the incorporation of longitudinal feedback. In addition, the limitations imposed on performance by large engine lags were found to be much less severe for systems with longitudinal feedback. The modifications suggested require a redesign of the approach power compensator system currently in use by the Navy.

TABLE OF CONTENTS

I. INTRODUCTION 8

A. APCS PERFORMANCE OBJECTIVES 8

B. AIRCRAFT 9

C. PREVIOUS STUDIES 9

D. OBJECTIVES 10

II. METHOD OF ANALYSIS 11

A. DESCRIPTION OF THE MODEL 11

B. DIGITAL SIMULATION 13

1. Continuous System Modeling Program 13

2. CSMP Program Components 13

C. THEORETICAL ANALYSIS 17

III. PROCEDURE 18

A. DIGITAL SIMULATION RUNS 18

B. ANALYSIS OF THE STANDARD APCS CONFIGURATION 19

C. INVESTIGATION OF ADDITIONAL APCS INPUTS 23

D. REVISED APCS CONFIGURATION 25

IV. DISCUSSION AND RESULTS 27

A. EFFECTS OF ENGINE RESPONSE 27

B. EFFECTS OF ADDITIONAL APCS INPUTS 28

1. Longitudinal Acceleration 28

2. Longitudinal Velocity 29

3. Proportional Plus Integral Longitudinal Velocity 29

4. Longitudinal Velocity Plus Acceleration 29

C. FINAL CONFIGURATION 30

TABLE OF CONTENTS (continued)

V. CONCLUSIONS AND RECOMMENDATIONS 32

A. APCS CONFIGURATION 32

B. ENGINE RESPONSE 33

C. THEORETICAL ANALYSIS 33

D. GENERALIZATION OF RESULTS 33

LIST OF REFERENCES 34

TABLES 35

FIGURES 44

APPENDIX A - CSMP COMPUTER PROGRAM AND SAMPLE OUTPUT 64

APPENDIX B - GUST MODEL ANALYSIS 77

APPENDIX C - MULTILOOP CONTROL SYSTEM ANALYSIS 83

INITIAL DISTRIBUTION LIST 89

FORM DD 1473 90

LIST OF TABLES

I. Aircraft Geometry and Stability Derivatives 35

II. Control Systems Parameters 36

III. CSMP Functional Blocks 37

IV. Aircraft State Equations Matrices 38

V. Aircraft Open Loop Transfer Function Numerators and Denominator 40

VI. Aircraft Transfer Function Numerators and Denominator for Standard APCS Loop Closures; T_e = 1.8 seconds 41

VII. RMS Velocity Error Summary 42

VIII. Aircraft Transfer Functions for Standard and Revised APCS Closures; T_e = 1.8 seconds 43

LIST OF FIGURES

1. Aircraft Equations of Motion 44

2. TF41-A-2 Engine Characteristics 45

3. Standard APCS Block Diagram 46

4. AFCS and ACLS Transfer Functions 47

5. Numerical Integration Error Analysis 47

6. Standard APCS Equivalent Block Diagram 48

7. Loci of Zeroes of Δ'' for $1/T_e$ Variation 49

8. Loci of Zeroes of $N^u_{\delta_e}]_{std}$ for $1/T_e$ Variation 50

9. Loci of Zeroes of $N^w_{\delta_e}]_{std}$ for $1/T_e$ Variation 51

10. Loci of Zeroes of $N^u_{u_g}]_{std}$ for $1/T_e$ Variation 52

11. Loci of Zeroes of Δ''' for $K_{\dot{u}}$ Variation 53

12. Loci of Zeroes of Δ''' for K_u Variation 54

13. Loci of Zeroes of Δ''' for K_u Variation, $K_p = 0.5$ 55

14. Loci of Zeroes of Δ''' for $K_{\dot{u}}$ Variation, $K_q = 0.2, 0.5, 1.0$ 56

15. Loci of Zeroes of $N^w_{\delta_e}]$ for $K_{\dot{u}}$ Variation, $K_q = 0.5$ 57

16. Revised APCS Equivalent Block Diagram 58

17. Loci of Zeroes of Δ''' for $1/T_e$ Variation, Revised Configuration 59

18. Loci of Zeroes of $N^w_{\delta_e}]_{rev}$ for $1/T_e$ Variation, Revised Configuration 60

19. Airspeed Response to Elevator, Bode Plot 61

20. Angle of Attack Response to Elevator, Bode Plot 62

21. Airspeed Response to Longitudinal Gust, Bode Plot 63

ACKNOWLEDGEMENT

The author wishes to thank Assistant Professor Ronald Hess for his guidance and assistance throughout the course of this research.

The patience and moral support shown by the author's wife, Jill, was greatly appreciated.

I. INTRODUCTION

A. APCS PERFORMANCE OBJECTIVES

The primary purpose of an approach power compensator system (APCS) in Navy carrier-based aircraft is to provide the thrust necessary to maintain the correct airspeed during carrier approach and landing. The APCS can be used either in an automatic carrier landing system (ACLS) or in a piloted, manual approach. Although airspeed systems exist [Ref. 1], the systems utilized in Navy aircraft attempt to maintain a constant angle of attack (AOA). Supplementary inputs, such as normal acceleration and elevator crossfeed, are usually employed in an effort to maintain the "on-speed" AOA. Since the on-speed value of AOA does not vary from approach to approach, there is no indexing requirement. In an airspeed system, however, the reference airspeed is a function of the aircraft configuration in the landing approach. As configuration variables, such as weight, vary from approach to approach, so does the reference airspeed. This is an important factor in favor of an AOA system. The pilot workload which airspeed indexing would add to an already demanding task probably would not be tolerated, and the designer of an approach power compensator system should bear this in mind.

Military specifications reflect the objective of maintaining a constant AOA. Reference 2 states that the output of the APCS shall be proportional to error in AOA, change in normal acceleration, integral of AOA error, and elevator position. As is noted in Ref. 1, it appears that the APCS design concept is overly restricted by military specifications. However, these specifications do point out the current Navy APCS concept.

B. AIRCRAFT

The aircraft chosen for study was the A-7E, a light-attack, carrier-based aircraft of approximately 20,000 pounds empty gross weight. The A-7E was chosen because it was one of two aircraft included in a previous study of Navy approach power compensator problems and requirements [Ref. 1] and because the author has had personal experience as an A-7A pilot.

The A-7E powerplant is a turbofan engine whose throttle response is characterized by a relatively long and nonlinear time constant in the approach thrust range. The APCS is an AOA system with inputs of AOA, integral of AOA, normal acceleration, and unit horizontal tail (UHT) movement. A detailed description of the system is contained in Ref. 3.

C. PREVIOUS STUDIES

Systems Technology, Incorporated conducted a study of Navy approach power compensator problems and requirements [Ref. 1]. The following is a summary of pertinent conclusions and recommendations:

1. A fundamental conceptual difficulty with current APCS's is the use of AOA feedback to constrain both AOA and airspeed, as the two are only in phase at low frequencies. Thus, it is possible to control only one of these or a linear combination of the two with a single control input. As a consequence, APCS design involves a compromise between these constraints.

2. Airframe characteristics restrict the ability to achieve satisfactory performance. Engine response time is a fundamental problem area, as the APCS cannot augment the dynamics without excessively overdriving the engine. It was recommended that the effect of engine lag on APCS performance be investigated in detail with a view toward specifying necessary characteristics.

3. Gust response within the current APCS concept will, in general, be poor. Gust proofing against longitudinal gusts with an AOA system is difficult. Gust proofing against vertical gusts has minimal effect, as the dominant response is determined by the short period characteristics.

4. It was recommended that the effects of additional feedbacks to the APCS be analyzed in relation to gust response and to optimum performance for separate configurations of fully automatic and manually controlled systems.

The Naval Air Test Center conducted an evaluation of the APCS in the A-7E [Ref. 3]. The emphasis was on optimizing the performance of the APCS for both manual and ACLS approaches with minimal material and design modifications. The recommended modifications were basically changes in feedback gains and the incorporation of a dual time constant in the UHT crossfeed circuit. A shorter time constant was used for nose up corrections than for nose down corrections, with the net result that the UHT input was more effective for nose up than for nose down attitude changes.

D. OBJECTIVES

The purpose of this research was to improve the performance of the APCS of the A-7E aircraft as used in the ACLS. Specifically, the effects of additional inputs to the APCS computer were evaluated with a goal of improving the current concept of APCS design. In addition, the effect of engine response time on APCS performance was determined.

II. METHOD OF ANALYSIS

A. DESCRIPTION OF THE MODEL

The fully automatic carrier landing mode was selected for study in this analysis of the APCS. The manual mode with the pilot in the loop was not considered. Thus, the total closed loop system consisted of the airframe, the engine, the approach power compensator, the longitudinal automatic flight control system (AFCS), and the automatic carrier landing system.

The aircraft equations of motion were linearized about the steady state approach conditions in accordance with standard small perturbation theory, as described by Etkin [Ref. 4]. Lateral-directional dynamics were not included. The resultant equations are shown in Figure 1. Aircraft stability derivatives and other parameter values were taken from Ref. 1 and are listed in Table I. Force and moment stability derivatives are normalized with respect to mass and moment of inertia, respectively. Hence, mass and moment of inertia do not appear explicitly in the equations of motion, as they do in Etkin's notation.

The A-7E engine is the TF41-A-2 turbofan. Reference 5 contains an analysis of the thrust-power lever relationship for a range of operating conditions. The nominal approach thrust for the operating conditions as shown in Table I is 3000 pounds. In this range of thrust, the engine response time constant is a nonlinear function of thrust. The relationship between the engine time constant, T_e, and thrust, and the relationship between thrust and power lever angle (δ_{PLA}) for the given operating conditions are taken from Ref. 1 and are shown in Figure 2. An average value of 275 pounds thrust per degree δ_{PLA} was used in the model. Thus, the variable engine lag was the only nonlinearity in the engine model.

Figure 3 is a schematic of the APCS loop closures. In small perturbation theory, AOA is defined as w/U_0, in radians. Thus, the inputs to the APCS computer are proportional plus integral w, a_z' (vertical acceleration corrected for accelerometer location), and a filtered UHT feedforward term.

The APCS gains are a representative set listed as "PAX" gains in Ref. 1 and do not correspond exactly to those in use in the current A-7E APCS configuration. In addition, several simplifications were made to the APCS model. A complex pole at ten rad/sec in the throttle actuator response was neglected. This frequency is well beyond the range in which the APCS is effective. Throttle linkage hysteresis of 0.5 degrees was ignored. The implementation of a dual UHT input time constant, as described in the introduction, was not incorporated into the model. A gain adjust bias exists in the APCS which changes all APCS gains by the same amount to compensate for ambient air temperature effects. The standard day value of 1.0 was used. K_{n_z}, the vertical acceleration gain, has two values, the smaller value being for load factors in excess of 1.1 g's. Only the larger value was incorporated into the model.

Both the longitudinal AFCS and the ACLS models were taken from Ref. 6. As above, the AFCS and ACLS gains were representative but were not necessarily identical to those currently in use. A complex pole and a first order lag at 20 rad/sec in the AFCS response was neglected. The AFCS output is a UHT deflection, which is a function of attitude error $(\theta-\theta_c)$, pitch rate, and normal acceleration. The automatic carrier landing system was represented by the A-7E SPN-42 longitudinal control equation. The output, a ship-to-aircraft pitch command, is a function of the aircraft altitude error, Z_e, measured perpendicular to the ideal

glide slope. In practice, the aircraft slant range and elevation are measured by the SPN-42 radar, corrected for ship motion and radar location, transformed into cartesian coordinates, and utilized to command an aircraft pitch angle.

The AFCS and ACLS longitudinal control equations are shown in Figure 4. APCS, AFCS, and ACLS gains are listed in Table II.

B. DIGITAL SIMULATION

1. Continuous System Modeling Program

The closed loop system was simulated on the IBM 360 digital computer utilizing a digital simulation language, CSMP. CSMP is an acronym for Continuous System Modeling Program. The program is augmented by basic FORTRAN and provides a set of functional blocks which simulate such analog components as integrators, relays, and function generators. A detailed description of the program is contained in Ref. 7. A description of CSMP functions used in the simulation is provided in Table III.

2. CSMP Program Components

A sample program and output are contained in Appendix A. The program consists of five major sections: the aircraft equations of motion and engine model, the APCS model, the AFCS model, the ACLS model, and a gust input model.

a. Aircraft Equations of Motion and Engine Model

The equations of motion as shown in Figure 1 were put into state format:

$$\begin{aligned} \{\dot{X}\} &= [A]\{X\} + [B]\{R\} \\ \{Y\} &= [C]\{X\} + [D]\{R\} + [E]\{Y\} \end{aligned} \qquad (1)$$

where:

$$\{X\} = \begin{Bmatrix} u \\ w \\ \theta \\ q \end{Bmatrix} \qquad \{Y\} = \begin{Bmatrix} \dot{h} \\ a_z \\ a'_z \end{Bmatrix} \qquad \{R\} = \begin{Bmatrix} \delta_e \\ \Delta T \\ u_g \\ w_g \end{Bmatrix} \quad (2)$$

The A, B, C, D, and E matrices are listed in Table IV.

The engine modeling consisted of two parts. As mentioned in section II.A., a relationship of 275 pounds thrust per degree δ_{PLA} was assumed. The engine time constant, as shown in Figure 2, was approximated by a linear function generator of fifteen unequally spaced points. The thrust operating range modeled was ±2000 pounds about the nominal operating value of 3000 pounds.

b. APCS Model

The APCS equations were obtained from Figure 3. The throttle actuator, power lever, and engine gains were combined into a single parameter. As a result, the variable labeled "PLA" in the CSMP program is not the actual power lever angle. Gains and other constants in the feedback loops were also consolidated wherever possible. AOA and integral of AOA were kept distinct. For ease of programming, the δ'_e/δ_e transfer function was written as

$$\frac{\delta'_e}{\delta_e}(s) = \frac{K_{\delta_e} T_w s}{T_w s+1} = \frac{1}{s + 1/T_w} \cdot K_{\delta_e} s \equiv \frac{W1}{\delta_e} \cdot \frac{\delta'_e}{W1} \quad (3)$$

The UHT input equations in the simulation are in the form of the right side of Equation (3).

c. AFCS Model

The AFCS equations were obtained from the equation given in Figure 4 with numerical values substituted for the various gains.

d. ACLS Model

The altitude error, Z_e, was defined as the negative of h, as the two are measured in opposite directions perpendicular to the ideal glideslope. The θ_c/Z_e transfer function, as shown in Figure 4, was rearranged for programming as follows:

$$\frac{\theta_c}{Z_e}(s) = \frac{K_c K_x}{K_p s+1}\left\{\left[\frac{\frac{s}{3.9}+1}{\left(\frac{s}{5}\right)^2+\frac{s}{3.5}+1}\right]\left[\frac{t_i K_x}{s}+1\right]+\left[\frac{R_x s}{\left(\frac{s}{5}\right)^2+\frac{s}{3.5}+1}\right]t_r\right\} \quad (4)$$

$$= K \cdot \frac{s^2+a_1 s+a_0}{s(s+1/K_p)(s^2+7.14s+25.0)}$$

where

$$K = \frac{K_c K_x (97.5 R_x t_r+25.0)}{3.9 K_p}$$

$$a_1 = \frac{3.9+t_i K_x}{3.9 R_x t_r+1.0} \qquad a_0 = \frac{3.9 t_i K_x}{3.9 R_x t_r+1.0}$$

Finally

$$\frac{\theta_c}{Z_e}(s) = \frac{K}{s} \cdot \frac{s^2+a_1 s+a_0}{s^3+b_2 s^2+b_1 s+b_0} \equiv \frac{Z_i}{Z_e} \cdot \frac{\theta_c}{Z_i} \quad (5)$$

where

$$b_2 = \frac{1}{K_p}+7.14 \qquad b_1 = \frac{7.14}{K_p}+25.0 \qquad b_0 = \frac{25.0}{K_p}$$

The SPN-42 equations in the simulation are in the form of the right side of Equation (5).

e. Gust Model

To simulate a random gust field, the output of a random number generator with a uniform amplitude distribution was passed through a second-order filter with a break frequency of 1.0 rad/sec and a damping ratio of 0.707. The theoretical derivation of the spectral properties of the resultant signal is described in Appendix B. Vertical and horizontal RMS gust velocities of 5.0 ft/sec were used in the simulation. To insure identical gust signals for each run, a constant step size was used in the numerical integrations for all runs.

f. RMS Velocity Error Criteria

An RMS velocity error for u and w was used as a measure of APCS effectiveness. It was defined as:

$$E_{RMS} = \left[\frac{1}{T} \int_0^T [u(t)^2 + w(t)^2] dt \right]^{\frac{1}{2}} \qquad (6)$$

where T is the run length.

g. Digital Simulation Error Analysis

A fourth-order Runge-Kutta numerical integration scheme with a fixed step size was used in the simulation. Figure 5 is a plot of normal acceleration after 0.5 seconds versus step size for an initial altitude error. Plots of other system variables, after 0.5 seconds and at other values of time, show the same trend. A step size of 0.05 seconds was chosen for the simulation.

C. THEORETICAL ANALYSIS

The theoretical analysis was primarily a root locus study of various APCS configurations. To reduce the multiple input, multiple output control system to a form adaptable to the analysis, a multiple loop analysis technique, documented in Ref. 8, was employed. An explanation of the method, including an example which covers all applications used in this study, is contained in Appendix C. Table V is a listing of the open loop aircraft numerators, cross product numerators, and the open loop denominator used in the analysis.

III. PROCEDURE

A. DIGITAL SIMULATION RUNS

A standard set of runs for the digital simulation was utilized for each configuration of the APCS. The APCS configuration shown in Figure 3 is referred to as the standard configuration. The length of the simulation runs was chosen to approximate the final approach phase of the carrier landing. Under SPN-42 control, two of the ACLS equation gains, R_x and K_x, are functions of range for a range greater than 6000 ft. For ranges less than 6000 ft. the values of R_x and K_x are constant at the values shown in Table II. The ACLS equation employed was valid for range less than 6000 ft. to the point at which deck motion compensation is introduced. A run time of 30 seconds was chosen to approximate this phase of the approach. A set of six standard simulation runs was chosen to simulate system response to initial high and low airspeed and altitude errors and to vertical and longitudinal gust inputs. The set of conditions for the six runs were:

Run (1) $u(0) = 5$ ft/sec, $w(0) = -5$ ft/sec

(2) $u(0) = -5$ ft/sec, $w(0) = 5$ ft/sec

(3) $Z_e(0) = 10$ ft

(4) $Z_e(0) = -10$ ft

(5) $\bar{u}_g = 5$ ft/sec

(6) $\bar{w}_g = 5$ ft/sec

Initial conditions and RMS gust velocities not specifically indicated in a run are zero.

B. ANALYSIS OF THE STANDARD APCS CONFIGURATION

To apply the analysis technique described in Section II.C, the APCS loop closures as shown in Figure 3 were reduced to an equivalent set that conformed to the block diagram format shown in Figure C.1. The equivalent transfer functions were a consolidation of all the elements in each loop closure, including the thrust to power lever terms. The resultant diagram is shown in Figure 6. G_w represents the proportional plus integral AOA feedback transfer function and is given by

$$G_w = -\frac{57.3 \cdot 1.389}{U_0}\left(\frac{K_\alpha}{T_\alpha s+1} + \frac{K_{\alpha_I}}{s}\right) \cdot \frac{350.7}{T_e(s+1/T_e)}$$

$$= \frac{-350.7 \cdot 57.3 \cdot 1.389\left(\frac{K_\alpha}{T_\alpha} + K_{\alpha_I}\right)\left(s + \frac{K_{\alpha_I}}{K_\alpha + K_{\alpha_I} T_\alpha}\right)}{U_0\, T_e s(s+1/T_\alpha)(s+1/T_e)} \qquad (7)$$

Numerically

$$G_w = -\frac{1021.5(s+0.197)}{T_e s(s+2.857)(s+1/T_e)}$$

G_z represents the normal acceleration feedback transfer function. The effect of the 6.7 ft. offset of the accelerometer on APCS performance has been shown to be minor in the low frequency range [Ref. 1]. Thus, the offset was neglected in the equivalent system, simplifying the analysis.

$$G_z = -\frac{K_{n_z} \cdot 350.7}{32.2 \cdot T_e(s+1/T_a)(s+1/T_e)} \qquad (8)$$

$$= -\frac{327.2}{T_e(s+1)(s+1/T_e)}$$

G_{δ_e} represents the UHT crossfeed transfer function and is given by

$$G_{\delta_e} = -\frac{K_{\delta_e} \cdot 350.7s}{T_e(s+1/T_w)(s+1/T_e)}$$

$$= -\frac{50,235s}{T_e(s+0.435)(s+1/T_e)} \tag{9}$$

The theoretical analysis was confined to the APCS loop closures only; AFCS and ACLS loop closures were not considered. Justification for this procedure is given in Section IV.B.

The closed loop transfer functions u/δ_e, w/δ_e, and u/u_g for the standard APCS configuration were formed. The engine time constant, T_e, was kept as a parameter, and root locus plots of the zeroes of the closed loop denominator and numerators were plotted to show the effects of engine lag.

Since there are two feedback paths, as shown in Figure 6, the closed loop denominator is defined as Δ''. It was derived by applying equation C.5.

$$\Delta'' = \Delta + G_w N^w_{\Delta T} + G_z N^{a_z}_{\Delta T} \tag{10}$$

$N^{a_z}_{\Delta T}$ was expanded as

$$N^{a_z}_{\Delta T} = N^{(sw-U_0 s\theta)}_{\Delta T} = sN^w_{\Delta T} - U_0 sN^\theta_{\Delta T} \tag{11}$$

Equation 11 was substituted into Equation 10 to yield

$$\Delta'' = \Delta + G_w N^w_{\Delta T} + sG_z(N^w_{\Delta T} - U_0 N^\theta_{\Delta T}) \tag{12}$$

The expression was cleared over a common denominator, and the numerator expressed in two terms, one a function of T_e, to give

$$\Delta'' = \frac{U + 1/T_e V}{s(s+1)(s+2.857)(s+1/T_e)} \tag{13}$$

where

$$U = s^2(s+1)(s+2.857)\Delta$$

$$V = s^7+4.913s^6+9.241s^5+10.91s^4+6.153s^3+1.240s^2 + 0.1810s-0.007699$$

The zeroes of Δ'' were plotted as a function of $1/T_e$ by forming an artificial transfer function, G, given by

$$G \equiv \frac{1/T_e V}{U} \tag{14}$$

G represents the open loop transfer function in a unity feedback, single loop system. This form was adaptable to a documented root locus digital computer program [Ref. 9]. The closed loop characteristic equation for the artificial system was

$$\Delta' = U + 1/T_e V \tag{15}$$

$1/T_e$ equal to zero represents an infinite engine lag, hence, a no thrust condition. Thus, the root loci originate at the open loop phugoid, short period, and control equation roots. The zeroes of the artificial closure represent the roots that would be obtained for the given APCS feedback gains if there were no engine delay. Figure 7 is a plot of the root loci. Only the loci above and on the real axis are shown. An

engine delay of 1.8 seconds occurs at the nominal operating thrust of 3000 pounds. This value and the values at thrust levels of ±2000 pounds about the nominal value are indicated on Figure 7.

Closed loop numerator zeroes were plotted for $N^u_{\delta_e}\Big]_{std}$, $N^w_{\delta_e}\Big]_{std}$, and $N^u_{u_g}\Big]_{std}$, where the subscript "std" refers to the loop closures for the standard configuration.

$$N^u_{\delta_e}\Big]_{std} = N^u_{\delta_e} + G_z N^{u\ a_z}_{\delta_e \Delta T} + G_w N^{u\ w}_{\delta_e \Delta T} + G_{\delta_e} N^u_{\Delta T}$$

$$= \frac{U + 1/T_e V}{s(s+1)(s+2.857)(s+0.435)(s+1/T_e)} \qquad (16)$$

where

$$U = s^2(s+1)(s+2.857)(s+0.435)N^u_{\delta_e}$$

$$V = -65.43s^7 - 318.6s^6 - 542.8s^5 - 1024.6s^4 - 718.8s^3$$

$$-87.79s^2 + 0.2346 + 1.707$$

Figure 8 is a plot of the zeroes of $N^u_{\delta_e}\Big]_{std}$ for $1/T_e$ variation.

$$N^w_{\delta_e}\Big]_{std} = N^w_{\delta_e} + G_w N^{w\ w}_{\delta_e \Delta T}\Big|_{0} + sG_z N^{w\ w}_{\delta_e \Delta T}\Big|_{0} - sG_z U_0 N^{w\ \theta}_{\delta_e \Delta T} + G_{\delta_e} N^w_{\Delta T}$$

$$= \frac{U + 1/T_e V}{s(s+1)(s+0.435)(s+1/T_e)} \qquad (17)$$

$$U = s(s+1)(s+0.435)N^{w}_{\delta_e}$$

$$V = -2.155s^5-511.6s^4-782.7s^3-343.6s^2-68.90s-8.753$$

Figure 9 is a plot of the zeroes of $N^{w}_{\delta_e}\Big]_{std}$ for $1/T_e$ variation.

$$N^{u}_{u_g}\Big]_{std} = N^{u}_{u_g} + G_w N^{u\ w}_{u_g}\Delta T + G_z N^{u\ a_z}_{u_g}\Delta T$$

$$= \frac{U + 1/T_e V}{s(s+2.857)(s+1)(s+1/T_e)} \qquad (18)$$

$$U = s^2(s+2.857)(s+1)N^{u}_{u_g}$$

$$V = 0.05453s^6+0.2789s^5+1.058s^4+1.716s^3+1.141s^2+1.797s-0.007686$$

Figure 10 is a plot of the zeroes of $N^{u}_{u_g}\Big]_{std}$ for $1/T_e$ variation.

C. INVESTIGATION OF ADDITIONAL APCS INPUTS

In studying the effects of additional APCS feedback variables, T_e was fixed at the nominal value of 1.8 seconds. The closed loop denominator and numerators evaluated at this value are shown in Table VI. The additional feedback variables which were considered were combinations of proportional, integral and derivative of longitudinal velocity, u. As a result, the closed loop u/u_g and u/δ_e transfer function zeroes were not affected. Subsequent to each root locus analysis, a set of digital simulation runs, as described in Section III.A, were completed with the altered configuration. A summary of the RMS velocity errors is contained in Table VII.

Longitudinal acceleration feedback was first considered. The equivalent transfer function for $\dot{u}$ feedback, defined as $G_{\dot{u}}$, is

$$G_{\dot{u}} \equiv \frac{350.7K_{\dot{u}}}{T_e(s+1/T_e)}$$

With T_e equal to 1.8 seconds, this becomes

$$G_{\dot{u}} = \frac{194.8K_{\dot{u}}}{s+0.56} \tag{19}$$

The closed loop denominator, defined as Δ''', was formed by modifying Δ'' as follows:

$$\Delta''' = \Delta'' + G_{\dot{u}}N^{su}_{\Delta T} \tag{20}$$

Figure 11 is a root locus plot of the zeroes of Δ''' as $K_{\dot{u}}$ was varied.

In a like manner, longitudinal velocity feedback was considered.

$$G_u \equiv \frac{194.8K_u}{s+0.56} \tag{21}$$

The closed loop denominator was again defined as Δ'''.

$$\Delta''' = \Delta'' + G_u N^{u}_{\Delta T} \tag{22}$$

Figure 12 is a plot of the zeroes of Δ''' as K_u was varied.

A combination of proportional plus integral longitudinal velocity was considered next.

$$G_{\hat{u}} \equiv \frac{194.8}{s+0.56} \cdot K_u(1+K_p/s) \tag{23}$$

Values of K_p from 0.1 to 0.5 were considered. Figure 13 is a plot of the zeroes of Δ''' as K_u was varied with K_p equal to 0.5.

The final configuration considered was proportional plus derivative of longitudinal velocity.

$$G_{\bar{u}} = \frac{194.8}{s+0.56} \cdot K_u^{\cdot}(s+K_q) \tag{24}$$

Figure 14 is a plot of the zeroes of Δ''' as $K_u^{\cdot}$ was varied with values of K_q equal to 0.2, 0.5, and 1.0. The phugoid roots are indicated for all three values of K_q. The closed loop numerator for the w/δ_e transfer function was formed.

$$N^w_{\delta_e}\Big]_{rev} = N^w_{\delta_e} + G_{\bar{u}} N^{w\ u}_{\delta_e} \Delta T \tag{25}$$

The subscript "rev" refers to revised configuration. The resultant root loci for K_q equal to 0.5 are shown in Figure 15.

D. REVISED APCS CONFIGURATION

Based on the results of the investigation of various inputs, a final APCS configuration was chosen. As compared to the standard system, this configuration had additional inputs of proportional plus derivative of longitudinal velocity with specific gains of 0.5 and 2.0 for K_q and $K_u^{\cdot}$, respectively. The revised equivalent APCS block diagram is shown in Figure 16.

With the gains fixed at the values given above, root locus plots for the zeroes of Δ''' and $N^w_{\delta_e}\Big]_{rev}$ for $1/T_e$ variation were plotted and are shown in Figures 17 and 18, respectively.

Straight-line approximations to Bode plots for u/δ_e, w/δ_e, and u/u_g were constructed for comparing the standard and revised APCS

configurations. The transfer functions are listed in Table VIII, and the magnitude portion of the Bode plots are shown in Figures 19 through 21.

IV. DISCUSSION AND RESULTS

A. EFFECTS OF ENGINE RESPONSE

Strictly speaking, the incremental root locus technique showing how the poles and zeroes of the APCS-equipped aircraft vary with the nonlinear engine time constant is not valid. The use of root locus analyses is valid only for linear systems. However, an incremental root locus technique has been used for stability analyses of systems with single-valued continuous nonlinearities [Ref. 10]. The system response is approximately defined by the instantaneous location of the roots, here a function of the instantaneous thrust.

The initial conditions and the gust inputs used in the simulation were considered to be representative of those that an APCS/aircraft system would be expected to encounter. Visual inspection of system response curves did not reveal the thrust response nonlinearity; i.e., the curves were approximately sinusoidal in shape, indicating that the system performance could be evaluated by considering a fixed value of T_e equal to 1.8 seconds. The minor effect of the nonlinearity was due to the low variance of ΔT in relation to the size of the thrust operating range modeled. The dependence of the response on T_e was greater for the revised system, as can be seen by comparing Figures 7 and 9 with Figures 17 and 18. This was a direct result of the increased capability to alter APCS performance with the longitudinal feedback.

The analysis did not provide insight concerning the specific effects of a large engine lag on APCS performance. However, the limitations imposed on performance by a large engine lag were shown to

be less severe for a system incorporating longitudinal feedback. As reported in Ref. 1, the larger feedback gains or lead compensation necessary to improve the standard AOA system performance result in excessively overdriving the engine. The longitudinal feedback provided an increase in performance and a more efficient use of the engine. The thrust response induced was directly related to the damped natural frequency of the phugoid mode. As the frequency was increased, as in Figure 12 for increasing K_u , peak to peak thrust values increased as well. However, for configurations in which the damped natural frequency was not appreciably increased, as in Figures 11 and 14, peak to peak thrust values were less than those for the standard configuration.

B. EFFECTS OF ADDITIONAL APCS INPUTS

As mentioned in Section III.B, the theoretical analysis neglected AFCS/ACLS loop closures. It was shown that these closures do not appreciably effect airspeed response for the system under study. Phugoid damping coefficients and damped natural frequencies were taken from the root locus plots of Figures 11 through 14. Measurements of the period and the time to one half initial amplitude of the airspeed responses were then made for the closed loop simulations, which included AFCS and ACLS closures. The damped frequencies and damping coefficients calculated from these responses were within a few per cent of those predicted by the root locus plots. Thus, it was concluded that airspeed response as controlled by the APCS was not significantly altered by AFCS and ACLS loop closures.

1. Longitudinal Acceleration

Only a limited increase in performance was achieved by the implementation of $\dot{u}$ feedback, as only a minimal increase in phugoid damping could be achieved.

2. Longitudinal Velocity

The addition of u feedback increased the absolute phugoid damping but provided only a minor increase in the damping coefficient and, therefore, no decrease in per cent overshoot. The most important factor was the increased damped natural frequency. It was considered necessary to keep the damped frequency near the level of that of the standard configuration, as a much higher value would prove unacceptable due to the rapid oscillations in thrust which would result.

3. Proportional Plus Integral Longitudinal Velocity

The inclusion of an integral term had an adverse effect on airspeed response for an initial airspeed error. This was predicted by the root locus plot as shown in Figure 13. The response to a longitudinal gust field was observed to be improved, as documented in Table VII. This shows up in the root locus plots of Figures 10 and 13 as an approximate cancellation of the phugoid poles with u/u_g zeroes.

4. Longitudinal Velocity Plus Acceleration

The inclusion of a combination of proportional plus derivative of longitudinal velocity in the APCS provided the best increase in overall system performance. For values of K_q greater than 0.5, the damped frequency increases substantially with the feedback gain, $K_{\dot{u}}$. For a value of K_q equal to 0.5 a large increase in damping was achieved while the damped frequency was held nearly constant. Improvement of APCS performance rapidly diminished as K_q was reduced below 0.5.

A stable first-order pole was shown to approach the origin as longitudinal feedback gains were increased [Figures 12 and 14], and its presence was evident in the digital simulations. For the configuration described in Section IV.B.4 with an initial airspeed error, a residual

airspeed error of opposite sign and with a value of ten per cent of the initial airspeed error remained and slowly decayed after the phugoid had essentially damped out. The effect of the pole was considered to be of minor significance. As shown in Figure 15, there was a corresponding zero in the w/δ_e numerator. Consequently, the first order pole did not appear in the angle of attack response.

C. FINAL CONFIGURATION

The choice of the final, revised configuration was based on several factors: phugoid damping, damped natural frequency and gust response. A combination of longitudinal velocity and acceleration inputs was the only combination able to provide a substantial increase in phugoid damping while maintaining a constant damped natural frequency. The choice of the value of K_u' was somewhat arbitrary. For a value of 2.0 the effective longitudinal velocity feedback gain was 1.0, which was of the same magnitude as K_α in units of volts per ft/sec; at a higher value of K_u' the airspeed input becomes dominant over AOA. Improved performance at a larger value of K_u' was indicated by the root locus plot and was verified by simulation [Table VII].

Longitudinal gust response was substantially improved for all configurations with longitudinal feedback. The most significant improvements, as indicated by the RMS velocity errors, were achieved for the configurations in which the damped natural frequency was increased over that of the standard configuration. The ratio of u to $\dot{u}$ feedback chosen represented a tradeoff between gust response and frequency criteria.

Vertical gust response as measured in simulation was not appreciably altered. As that was expected prior to the study (Section I.C), there was no theoretical analysis attempted in that area.

For an initial altitude error for all configurations, the induced airspeed error was primarily an AOA, or w(t), transient which decays in five seconds. The induced airspeed error, u(t), was much smaller in comparison. Thus, the addition of the longitudinal feedbacks have a negligible effect on responses induced by an initial altitude error. Based on this result, it was concluded that airspeed response at push-over from level flight to glideslope acquisition would be unaltered.

The frequency response plots of Figures 19 through 21 indicate the frequency range which was modified by the APCS revision. The amplitude plots for u/δ_e and u/u_g indicate this range was from 0.07 to 0.5 rad/sec, while only the amplitudes at low frequencies were attenuated in the w/δ_e plot. The additional favorable effect of an approximate three dB attenuation at the phugoid break frequency of the revised configuration was not indicated on the asymptotic plots.

V. CONCLUSIONS AND RECOMMENDATIONS

A. APCS CONFIGURATION

Substantial improvement in performance is possible through the use of longitudinal feedback. However, only an acceleration term can be practically obtained with the current APCS, as it would entail only the implementation of an accelerometer signal. Once an airspeed feedback is considered, the need for an airspeed reference is required, necessitating a major APCS redesign. An airspeed reference, manually set by the pilot, would not be acceptable. In addition to the added pilot responsibility mentioned in Section I, the combined AOA/airspeed system references would require airspeed reference accuracy greater than the pilot could be expected to provide.

In summary, only limited improvement in performance is possible within current limitations. It is recommended that the current APCS design concept be considered for revision. Present day aircraft, such as the A-7E and the F-14A/B, have precise airspeed measuring equipment (air data computers) and digital computers on board. The possibility of utilizing those devices to accurately measure and reference airspeed for its incorporation into the APCS should be studied.

The possible improvement of gust response gained by the revised APCS configuration is partially governed by the method of sensing airspeed. If an inertial device is utilized, the actual airspeed, u, is measured, but the term $(u-u_g)$ is measured if an air data computer is utilized. The effect of including the gust velocity in the sensed airspeed signal was to degrade performance below that gained by the revised configuration (e.g., the RMS value of velocity error for a

horizontal gust input was 4.1 ft/sec. With the gust velocity included in the feedback signal, the error was 5.0 ft/sec, still substantially improved over the original value of 6.3 ft/sec).

Angle of attack response was not degraded by the inclusion of longitudinal feedback but, in fact, was improved.

B. ENGINE RESPONSE

The effect of the nonlinear engine time constant on APCS performance was shown to be minor for the range of operating conditions considered.

The limitations imposed on APCS performance by a large engine lag are much less severe for a system incorporating longitudinal velocity and acceleration feedback than for the standard angle of attack configuration.

C. THEORETICAL ANALYSIS

Restricting the multiple loop control system analysis technique to the APCS loop closures was shown to be valid for an evaluation of airspeed control. The implementation of the method provided a systematic approach for the study of APCS performance.

D. GENERALIZATION OF RESULTS

The choice of a single APCS/aircraft system for the analysis may restrict the validity of some of the results to that particular system. However, as all current Navy APCS's use the same basic AOA system, it is postulated that the general concept presented is applicable to other aircraft. Correlation of results with other systems should be attempted.

The study was restricted to the fully automated carrier landing mode. The validity of the results for a pilot-controlled attitude loop should be investigated.

REFERENCES

[1] Systems Technology, Inc. Report 197-1, An Analysis of Navy Approach Power Compensator Problems and Requirements, by S. J. Craig, R. F. Ringland, and I. L. Ashkenas, March 1971.

[2] Department of the Navy Military Specification MIL-23866A(WP), Control Set, Approach Power AN/ASN-54 (V), 15 September 1965.

[3] Naval Air Test Center Report FT-16R-71, Evaluation of the Approach Power Compensator System in the A-7E Airplane, by Lcdr W. C. Bowes, USN, A. P. Schust, Jr., and J. L. Griffith, 19 March 1971.

[4] Etkin, B., Dynamics of Flight, Wiley, 1959.

[5] Naval Air Propulsion Test Center Report ATD-211, TF41-A-2 Engine Thrust-Power Lever Relationship, by P. F. Piscopo, January 1972.

[6] Naval Air Test Center Report FT-28R-72, Development of the A-7E Airplane Automatic Carrier Landing System (ACLS) Mode I Operational Capability, by Lt W. B. Christie, USN and A. P. Schust, Jr., 11 May 1972.

[7] IBM Application Program 360A-CX-16X, System/360 Continuous System Modeling Program User's Manual, 4th ed.,IBM Corporation, October 1969.

[8] Air Force Flight Dynamics Laboratory Report TDR-62-1014, Analysis of Multiloop Vehicular Control Systems, by D. T. McRuer, I. L. Ashkenas, and H. R. Pass, March 1964.

[9] Air Force Flight Dynamics Laboratory Report FDCC TM 69-4, User's Manual for a Digital Computer Routine to Calculate Root Loci, by F. L. George and Capt J. D. Fisher, USAF, December 1969, Revised October 1971.

[10] Thaler, G. H., DR. ENG. and Pastel, M. P., Ph.D. Analysis and Design of Nonlinear Feedback Control Systems, McGraw Hill, 1962.

TABLE I

AIRCRAFT GEOMETRY AND STABILITY DERIVATIVES

STABILITY DERIVATIVES		APPROACH PARAMETERS	
X_u	- 0.05435	S	375 ft^2
X_w	0.064327	W	24,000 lb
Z_u	- 0.286953	I_{yy}	68,000 slug-ft^2
$Z_{\dot{w}}$	0	MAC	10.84 ft
Z_w	- 0.528871	m	746 slugs
M_u	- 0.000165	h	Sea Level
$M_{\dot{w}}$	- 0.000289	ρ	0.002378 $\frac{slugs}{ft^3}$
M_w	- 0.007964	U_0	218 ft/sec
M_q	- 0.327532	α_0	12 deg
X_{δ_e}	0.732836	c.g.	28.6 % MAC
Z_{δ_e}	-14.713536	l_x	6.7 ft (ahead of c.g.)
M_{δ_e}	- 2.188878		
$X_{\Delta T}$	0.001317		
$Z_{\Delta T}$	- 0.000250		
$M_{\Delta T}$	0.000004		

TABLE II

CONTROL SYSTEMS PARAMETERS

AFCS

K_θ	1.9	rad/rad
$K_{\dot{\theta}}$	1.0	rad/rad-sec
K_{n_z}	3.0	deg/g

ACLS

K_c	1/5.4
K_x	1.0
K_p	0.376
R_x	1.0
t_i	1/15
t_r	2.5

APCS

K_{δ_e}	143.2	volts/rad
T_w	2.3	sec
K_α	2.6	volts/unit α
K_{α_I}	0.55	volts/unit-sec
T_α	0.35	sec
K_{n_z}	30.0	volts/g
T_a	1.0	sec

TABLE III

CSMP FUNCTIONAL BLOCKS

General Form	Function
Y = INTGRL(IC,X) Y(0) = IC Integrator	$Y = \int_0^t X dt + IC$ Laplace Transform: $\frac{1}{s}$
Y = REALPL(IC,P,X) Y(0) = IC 1^{st} Order Lag	$P\dot{Y} + Y = X$ Laplace Transform: $\frac{1}{Ps + 1}$
Y = CMPXPL(IC_1,IC_2,P_1,P_2,X) $Y(0) = IC_1$ $\dot{Y}(0) = IC_2$ Complex Pole	$\ddot{Y} + 2P_1P_2\dot{Y} + P_2^2Y = X$ Laplace Transform: $\frac{1}{s^2 + 2P_1P_2s + P_2^2}$
Y = AFGEN(FUNCT,X) Arbitrary Function Generator(Linear Interpolation)	Y = FUNCT(X)
Y = RNDGEN(P) P = ANY ODD INTEGER NOISE(RANDOM NUMBER) GENERATOR WITH A UNIFORM DISTRIBUTION	UNIFORM DISTRIBUTION OF VARIABLE Y p(Y) = Probability distribution Function: 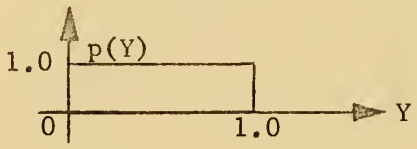

TABLE IV

AIRCRAFT STATE EQUATIONS MATRICES

[A]

$$\begin{bmatrix} X_u & X_w & -g & 0 \\ \frac{Z_u}{1-Z_{\dot{w}}} & \frac{Z_w}{1-Z_{\dot{w}}} & 0 & U_0 \\ 0 & 0 & 0 & 1.0 \\ M_u+\frac{M_{\dot{w}}Z_u}{1-Z_{\dot{w}}} & M_w+\frac{M_{\dot{w}}Z_w}{1-Z_{\dot{w}}} & 0 & M_q+\frac{M_{\dot{w}}U_0}{1-Z_{\dot{w}}} \end{bmatrix}$$

[B]

$$\begin{bmatrix} X_{\delta_e} & X_{\Delta T} & -X_u & -X_w \\ Z_{\delta_e} & Z_{\Delta T} & -Z_u & -Z_w \\ 0 & 0 & 0 & 0 \\ M_{\delta_e}+\frac{M_{\dot{w}}Z_{\delta_e}}{1-Z_{\dot{w}}} & M_{\Delta T}+\frac{M_{\dot{w}}Z_{\Delta T}}{1-Z_{\dot{w}}} & -M_u-\frac{M_{\dot{w}}Z_u}{1-Z_{\dot{w}}} & -M_w-\frac{M_{\dot{w}}Z_w}{1-Z_{\dot{w}}} \end{bmatrix}$$

TABLE IV (continued)

$$[C]$$

$$\begin{bmatrix} 0 & -1.0 & U_0 & 0 \\ \frac{Z_u}{1-Z_{\dot{w}}} & Z_w & 0 & 0 \\ -1'_x\left(M_u + \frac{M_w Z_u}{1-Z_{\dot{w}}}\right) & -1_x\left(M_w + \frac{M_{\dot{w}} Z_w}{1-Z_{\dot{w}}}\right) & 0 & -1_x\left(M_q + \frac{M_{\dot{w}} U_0}{1-Z_{\dot{w}}}\right) \end{bmatrix}$$

$$[D]$$

$$\begin{bmatrix} 0 & 0 & 0 & 0 \\ Z_{\delta_e} & Z_{\Delta T} & -Z_u & -Z_w \\ -1_x\left(M_{\delta_e} + \frac{M_{\dot{w}} Z_{\delta_e}}{1-Z_{\dot{w}}}\right) & -1_x\left(M_{\Delta T} + \frac{M_{\dot{w}} Z_{\Delta T}}{1-Z_{\dot{w}}}\right) & 1_x\left(M_u + \frac{M_{\dot{w}} Z_u}{1-Z_{\dot{w}}}\right) & 1_x\left(M_w + \frac{M_{\dot{w}} Z_w}{1-Z_{\dot{w}}}\right) \end{bmatrix}$$

$$[E]$$

$$\begin{bmatrix} 0 & 0 & 0 \\ 0 & 0 & 0 \\ 0 & 1.0 & 0 \end{bmatrix}$$

TABLE V

AIRCRAFT OPEN LOOP TRANSFER FUNCTION

NUMERATORS AND DENOMINATOR

$$\Delta = s^4 + 0.973939s^3 + 1.97797s^2 + 0.109846s + 0.070689$$

$$N^{w}_{\Delta T} = -0.00025s^3 + 0.0003986s^2 - 0.0001281s + 0.00003824$$

$$N^{\theta}_{\Delta T} = 0.00000407s^2 + 0.00000422s + 0.00000320s$$

$$N^{u}_{\Delta T} = 0.001317s^3 + 0.001195s^2 + 0.002435s - 0.0001321$$

$$N^{w}_{\delta_e} = -14.7135s^3 - 483.007s^2 - 26.3803s - 20.1217$$

$$N^{u}_{\delta_e} = 0.732836s^3 - 0.272704s^2 + 40.6515s + 33.4610$$

$$N^{u}_{u_g} = 0.054534s^3 + 0.0685976s^2 + 0.109846s + 0.070689$$

$$N^{u\ w}_{\delta_e \Delta T} = 0.0191945s^2 + 0.635365s - 0.0194913$$

$$N^{u\ \theta}_{\delta_e \Delta T} = 0.00288013s + 0.0013343$$

$$N^{w\ u}_{\delta_e \Delta T} = -0.0191945s^2 - 0.635365s + 0.0194913$$

$$N^{w\ \theta}_{\delta_e \Delta T} = -0.00060607s - 0.00085794$$

$$N^{u\ w}_{u_g \Delta T} = -0.00039155s^2 - 0.00012806s + 0.00003824$$

$$N^{u\ \theta}_{u_g \Delta T} = 0.0000001131s + 0.00000320$$

TABLE VI

AIRCRAFT TRANSFER FUNCTION NUMERATORS AND DENOMINATOR FOR STANDARD APCS LOOP CLOSURES

T_e = 1.8 SECONDS

$$\Delta'' = \frac{1}{s(s+1)(s+2.857)(s+0.56)}\Big\{[0.303,0.278](-0.263)(0.032)(-1.099)[0.346,1.44](-2.89)\Big\}$$

$$\left[N^{u}_{\delta_e}\right]_{std} = \frac{0.7328}{s(s+1)(s+2.857)(s+0.435)(s+0.56)}\Big\{[0.504,0.182](0.150)[-0.176,1.38](-0.807)(-3.41)(49.5)\Big\}$$

$$\left[N^{w}_{\delta_e}\right]_{std} = \frac{-14.71}{(s+1)(s+0.435)(s+0.56)}\Big\{[0.389,0.257](-0.253)(-0.584)(-1.05)(-32.2)\Big\}$$

$$\left[N^{u}_{u_g}\right]_{std} = \frac{0.5453}{s(s+1)(s+2.857)(s+0.56)}\Big\{[0.308,0.716](0.00948)[0.0836,1.74](-1.58)(-3.37)\Big\}$$

Notation: $[\zeta\ ,\ \omega_n]$ represents $(s^2+2\zeta\omega_n+\omega_n^{\,2})$

(τ) represents $(s-\tau)$

positive ζ and negative τ represent stable roots

TABLE VII

RMS VELOCITY ERROR SUMMARY

APCS Configuration	u_0= 5 w_0=-5	u_0=-5 w_0= 5	Z_{e_0}=10	Z_{e_0}=-10	$\bar{w}_g$=5	$\bar{u}_g$=5
Standard	3.09	2.87	3.14	3.06	7.40	6.26
Long Accel						
$K_u^{\cdot}$=1.0	3.02	2.85	3.08	3.03	7.01	5.63
K_u=2.0	3.03	2.91	3.05	3.01	6.75	5.28
=3.0	3.09	3.00	3.03	2.96	6.57	5.05
Long Veloc						
K_u=1.0	2.78	2.57	3.09	3.05	7.11	4.16
K_u=2.0	2.69	2.38	3.05	3.03	6.72	3.44
=3.0	2.59	2.20	3.01	3.01	6.40	3.28
Prop+Int u						
$K_u(u+\frac{1}{2}\int u)$						
K_u=1.0	3.26	2.95	3.16	3.11	7.79	4.46
K_u=3.0	3.88	3.05	3.10	3.11	6.23	3.30
Prop+Accel u						
$K_u^{\cdot}(\dot{u}+K_q u)$						
K_q=1.0						
$K_u^{\cdot}$=1.0	2.65	2.48	3.05	3.02	6.76	4.07
=3.0	2.35	2.30	2.99	2.98	6.18	3.55
K_q=0.5						
$K_u^{\cdot}$=1.0	2.75	2.60	3.07	3.02	6.87	4.61
=2.0*	2.61	2.48	3.03	3.00	6.55	4.06
=3.0	2.52	2.41	3.01	2.96	6.35	3.84
K_q=0.2						
$K_u^{\cdot}$=1.0	2.88	2.72	3.07	3.03	6.94	5.12
=3.0	2.73	2.64	3.02	2.99	6.46	4.33

* Underlined values denote revised configuration.

TABLE VIII

AIRCRAFT TRANSFER FUNCTIONS FOR STANDARD AND REVISED APCS CLOSURES; T_e = 1.8 SECONDS

$$\frac{u}{\delta_e}(s)_{std} = \frac{0.733[0.504,0.182](0.150)(-0.807)[-0.176,1.38](-3.41)(49.5)}{(-0.435)[0.303,0.278](-0.263)(0.0320)(-1.099)[0.346,1.44](-2.89)}$$

$$\frac{u}{\delta_e}(s)_{rev} = \frac{0.733[0.504,0.182](0.150)(-0.807)[-0.176,1.38](-3.41)(49.5)}{(-0.435)[0.764,0.514](-0.0630)(-1.15)(0.0372)[0.361,1.44](-2.90)}$$

$$\frac{w}{\delta_e}(s)_{std} = \frac{-14.7(-0.253)[0.389,0.257](-0.584)(-1.05)(-32.3)(0.0)(-2.857)}{(-0.435)[0.303,0.278](-0.263)(0.0320)(-1.099)[0.346,1.44](-2.89)}$$

$$\frac{w}{\delta_e}(s)_{rev} = \frac{-14.7(-0.660)[0.880,0.458](-0.0447)(-1.094)(-32.2)(0.0)(-2.857)}{(-0.435)[0.764,0.514](-0.0630)(-1.15)(0.0372)[0.361,1.44](-2.90)}$$

$$\frac{u}{u_g}(s)_{std} = \frac{0.0545[0.308,0.716](0.00948)[0.0836,1.74](-1.58)(-3.37)}{[0.303,0.278](-0.263)(0.0320)(-1.099)[0.346,1.44](-2.89)}$$

$$\frac{u}{u_g}(s)_{rev} = \frac{0.0545[0.308,0.716](0.00948)[0.0836,1.74](-1.58)(-3.37)}{[0.764,0.514](-0.0630)(-1.15)(0.0372)[0.361,1.44](-2.90)}$$

Notation: $[\zeta, \omega_n]$ represents $(s^2 + 2\zeta\omega_n s + \omega_n^2)$; (τ) represents $(s-\tau)$; positive ζ and negative τ represent stable roots.

$$
\begin{bmatrix}
s-X_u & -X_w & g & 0 & 0 & 0 \\
-Z_u & (1-Z_{\dot{w}})s-Z_w & -U_0 s & 0 & 0 & 0 \\
-M_u & -(M_{\dot{w}}s+M_w) & s^2-M_q s & 0 & 0 & 0 \\
0 & 1 & -U_0 & 1 & 0 & 0 \\
0 & -s & U_0 s & 0 & 1 & 0 \\
0 & -s & 1_x s^2+U_0 s & 0 & 0 & 1
\end{bmatrix}
\begin{bmatrix} u \\ w \\ \theta \\ \dot{h} \\ a_z \\ a_z' \end{bmatrix}
=
\begin{bmatrix}
X_{\delta_e} & X_{\Delta T} & -X_u & -X_w \\
Z_{\delta_e} & Z_{\Delta T} & -Z_u & -Z_w \\
M_{\delta_e} & M_{\Delta T} & -M_u & -M_w \\
0 & 0 & 0 & 0 \\
0 & 0 & 0 & 0 \\
0 & 0 & 0 & 0
\end{bmatrix}
\begin{bmatrix} \delta_e \\ \Delta T \\ u_g \\ w_g \end{bmatrix}
$$

FIGURE 1. AIRCRAFT EQUATIONS OF MOTION

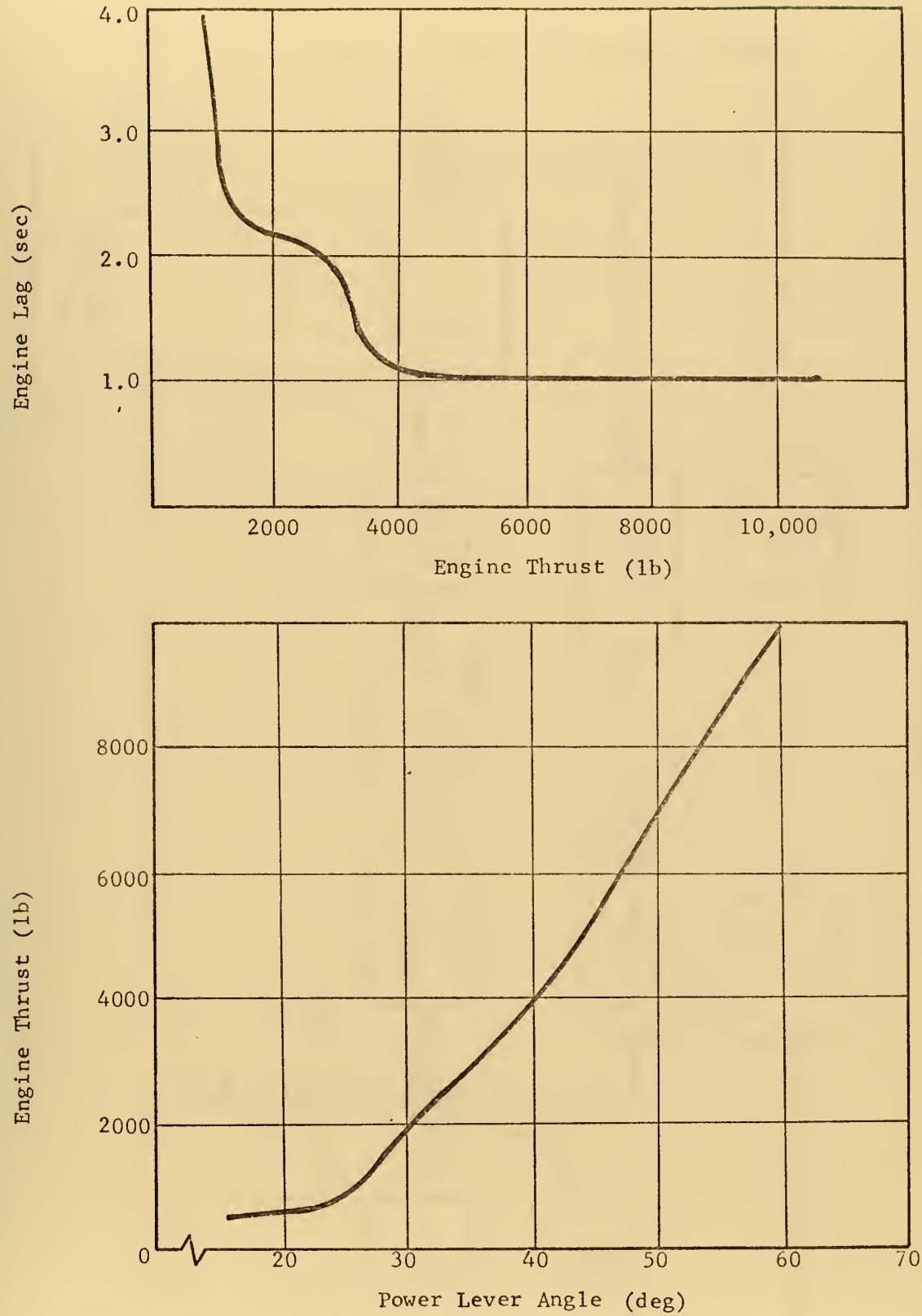

FIGURE 2. TF41-A-2 ENGINE CHARACTERISTICS

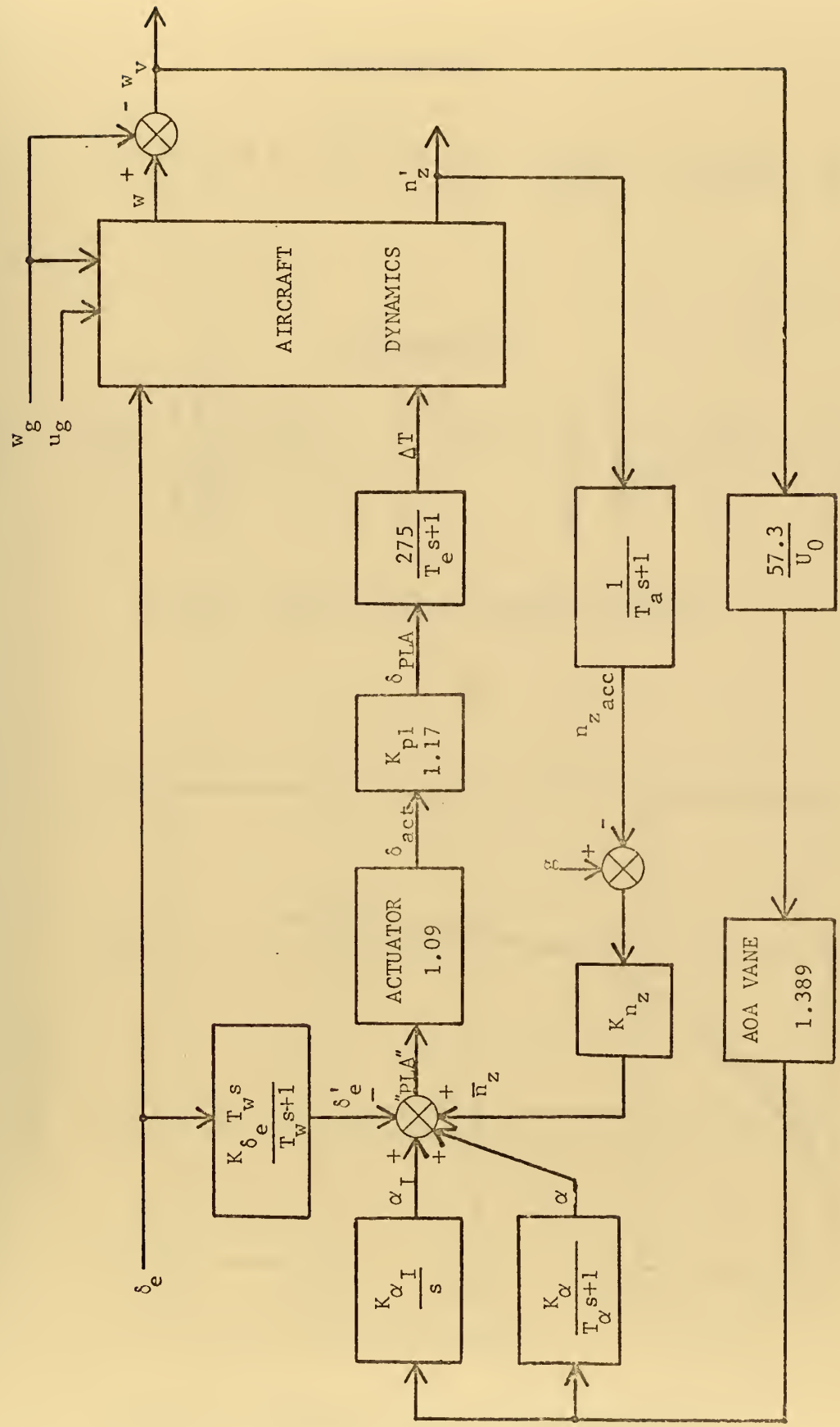

FIGURE 3. STANDARD APCS BLOCK DIAGRAM

AFCS EQUATION

$$\delta_e = \left[K_\theta(\theta-\theta_c)+K_{\dot\theta}\dot\theta + \frac{K_{n_z} N_z}{0.55s + 1}\right] \left[\frac{1}{\left(\frac{s}{20} + 1\right)\left[\left(\frac{s}{20}\right)^2 + \frac{2(0.7)s}{20} + 1\right]}\right]$$

ACLS EQUATION

$$\frac{\theta_c}{Z_e} = \frac{K_c K_x}{K_p s+1} \left\{\left[\frac{\frac{s}{3.9} + 1}{\left(\frac{s}{5}\right)^2 + \frac{s}{3.5} + 1}\right] \left[\frac{t_i K_x}{s} + 1\right] + \left[\frac{R_x s}{\left(\frac{s}{5}\right)^2 + \frac{s}{3.5} + 1}\right] t_r\right\}$$

FIGURE 4. AFCS AND ACLS TRANSFER FUNCTIONS

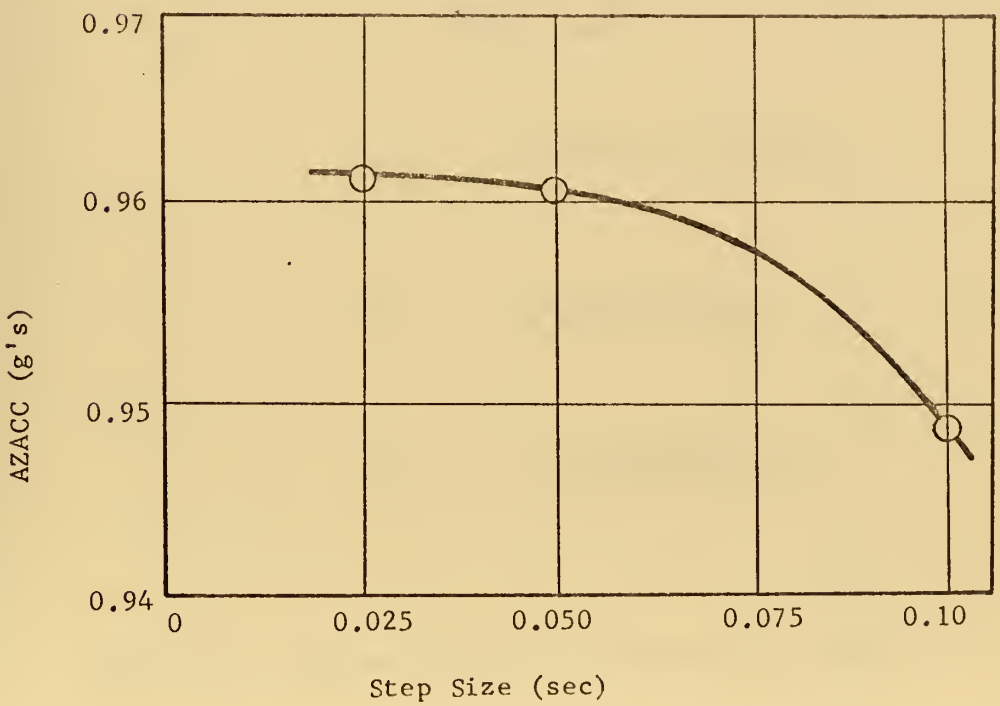

FIGURE 5. NUMERICAL INTEGRATION ERROR ANALYSIS

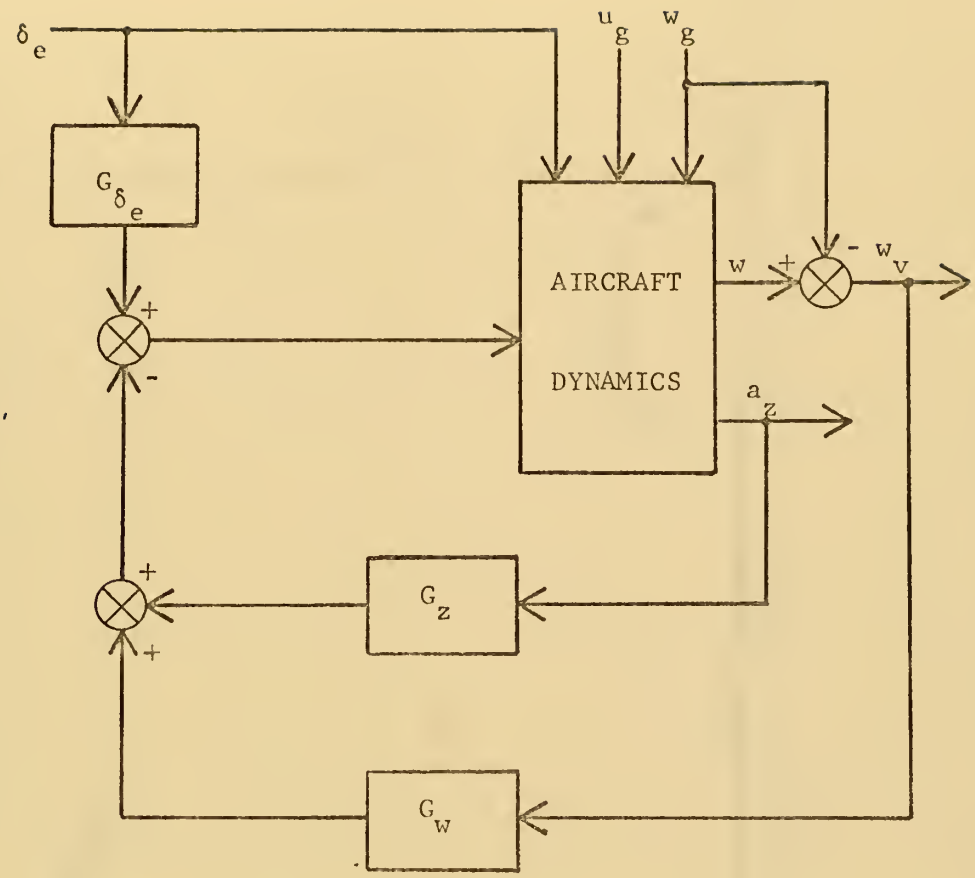

$$G_w = - \frac{1021.5(s+0.197)}{T_e s(s+2.857)(s+1/T_e)}$$

$$G_z = - \frac{327.2}{T_e(s+1)(s+1/T_e)}$$

$$G_{\delta_e} \doteq - \frac{50,235s}{T_e(s+0.435)(s+1/T_e)}$$

FIGURE 6. STANDARD APCS EQUIVALENT BLOCK DIAGRAM

FIGURE 7. LOCI OF ZEROES OF Δ'' FOR $1/T_e$ VARIATION

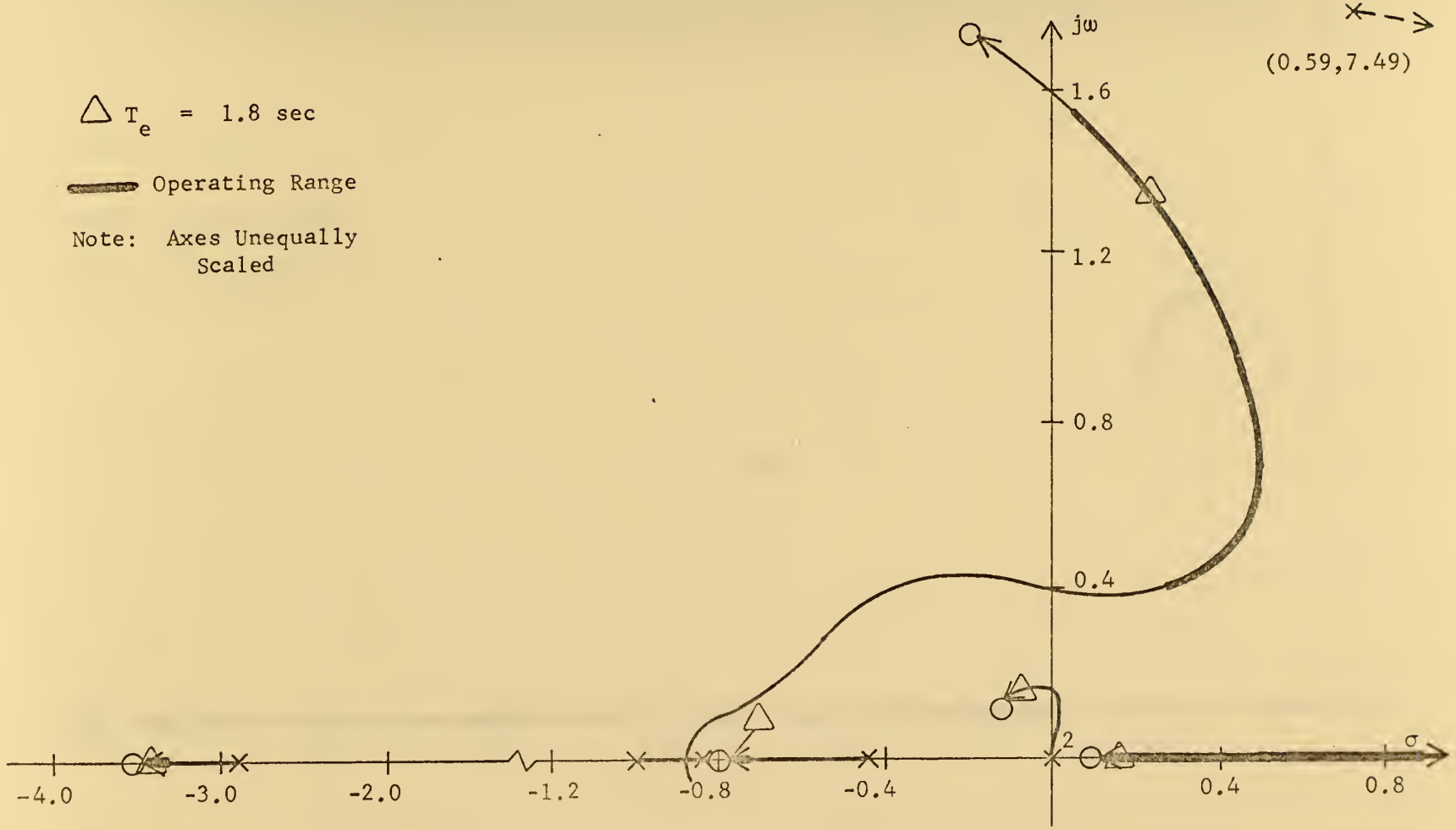

FIGURE 8. LOCI OF ZEROES OF $N^{u}_{\delta_e}\Big]_{std}$ FOR $1/T_e$ VARIATION

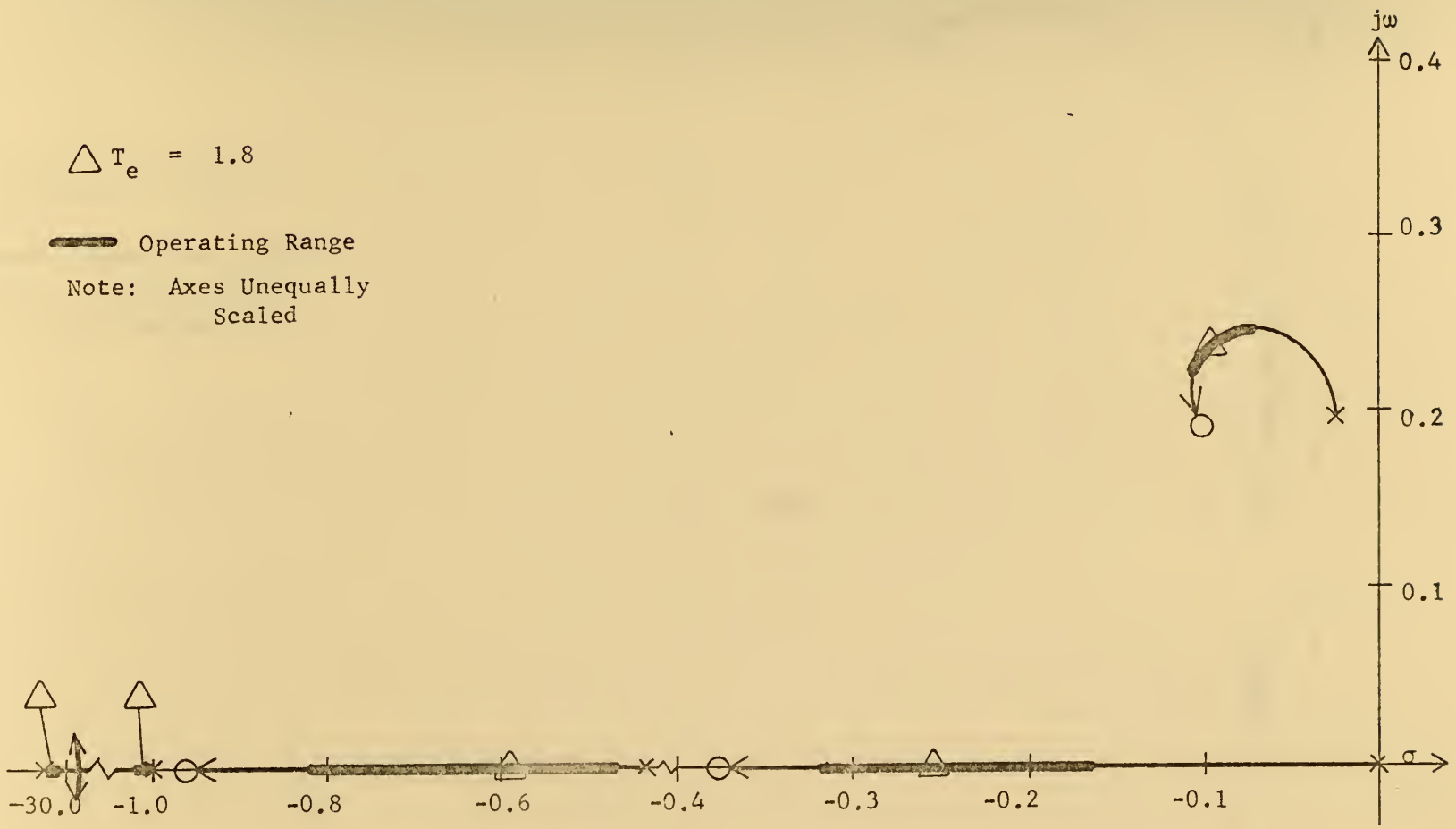

FIGURE 9. LOCI OF ZEROES OF $N^{w}_{\delta_e}\Big]_{std}$ FOR $1/T_e$ VARIATION

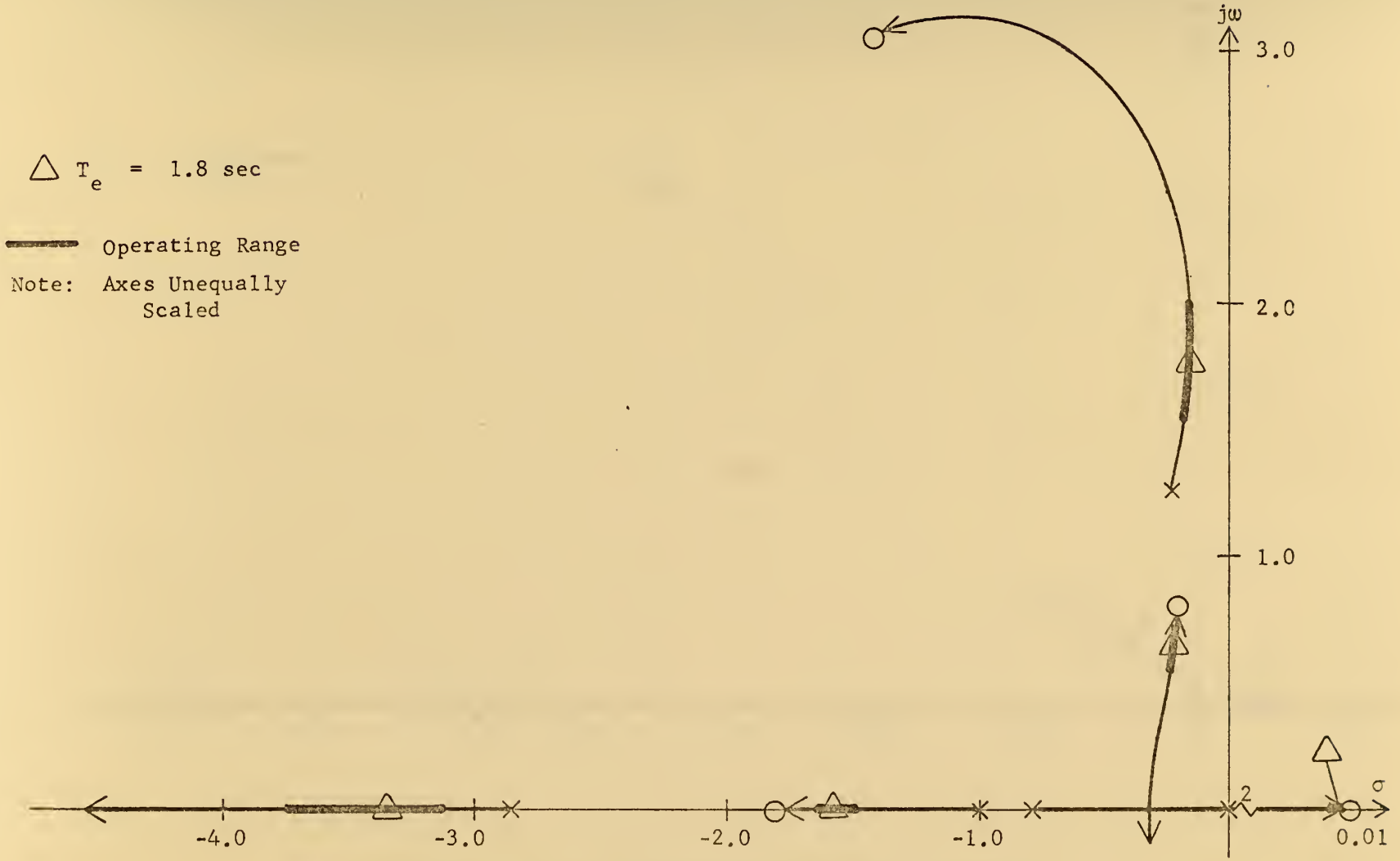

FIGURE 10. LOCI OF ZEROES OF $\left[N^{u}_{u_g}\right]_{std}$ FOR $1/T_e$ VARIATION

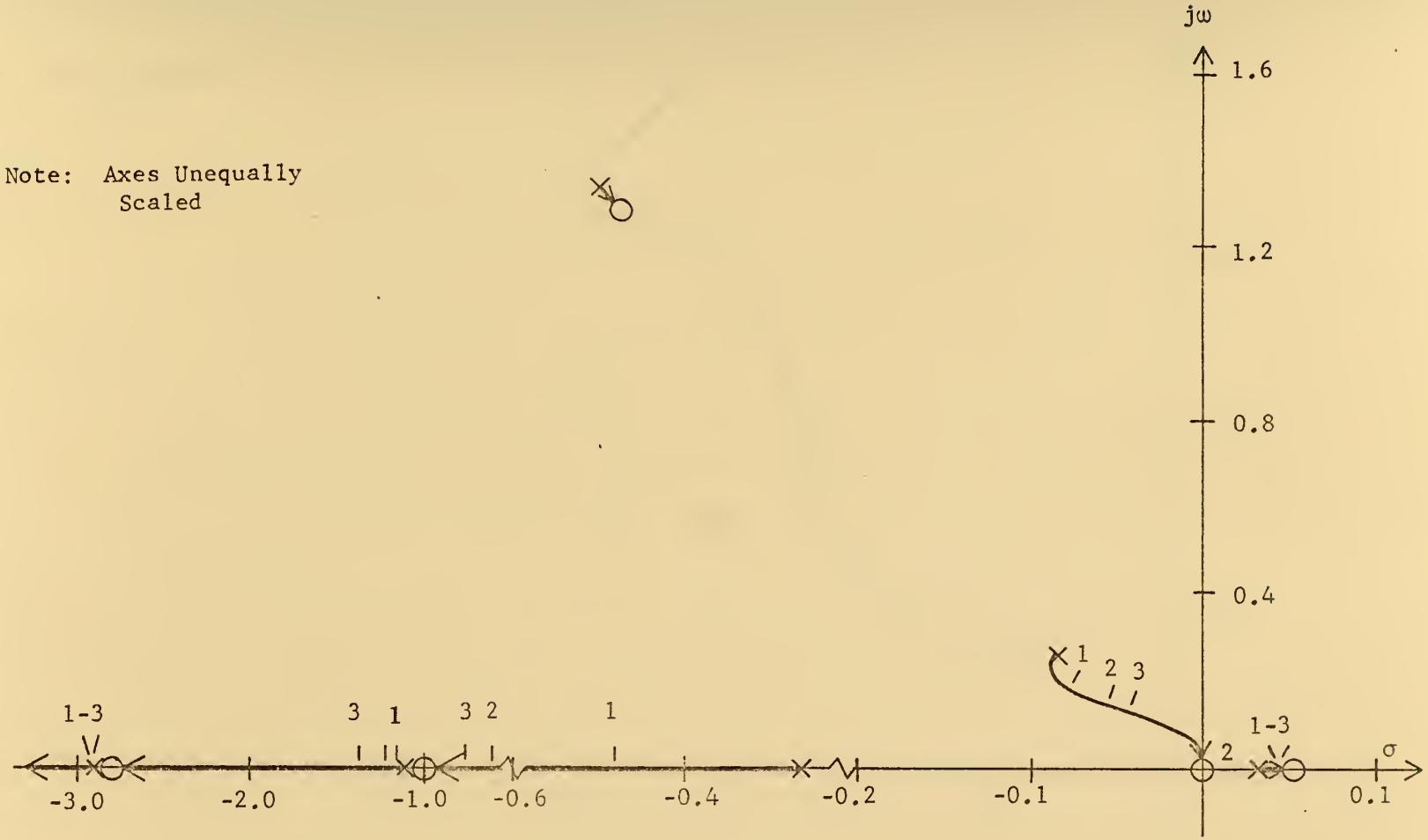

FIGURE 11. LOCI OF ZEROES OF Δ''' FOR K_u VARIATION

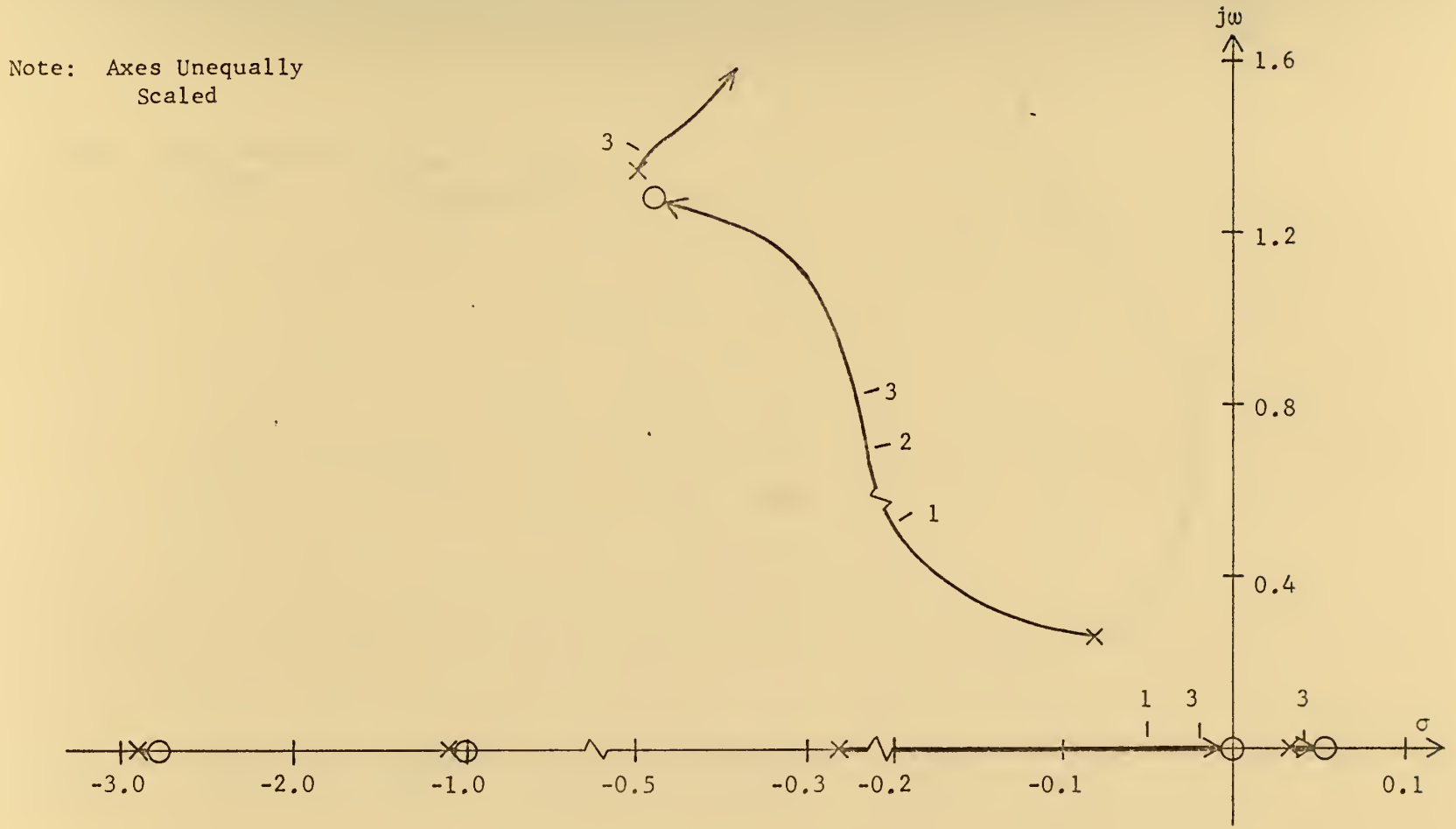

FIGURE 12. LOCI OF ZEROES OF Δ''' FOR K_u VARIATION

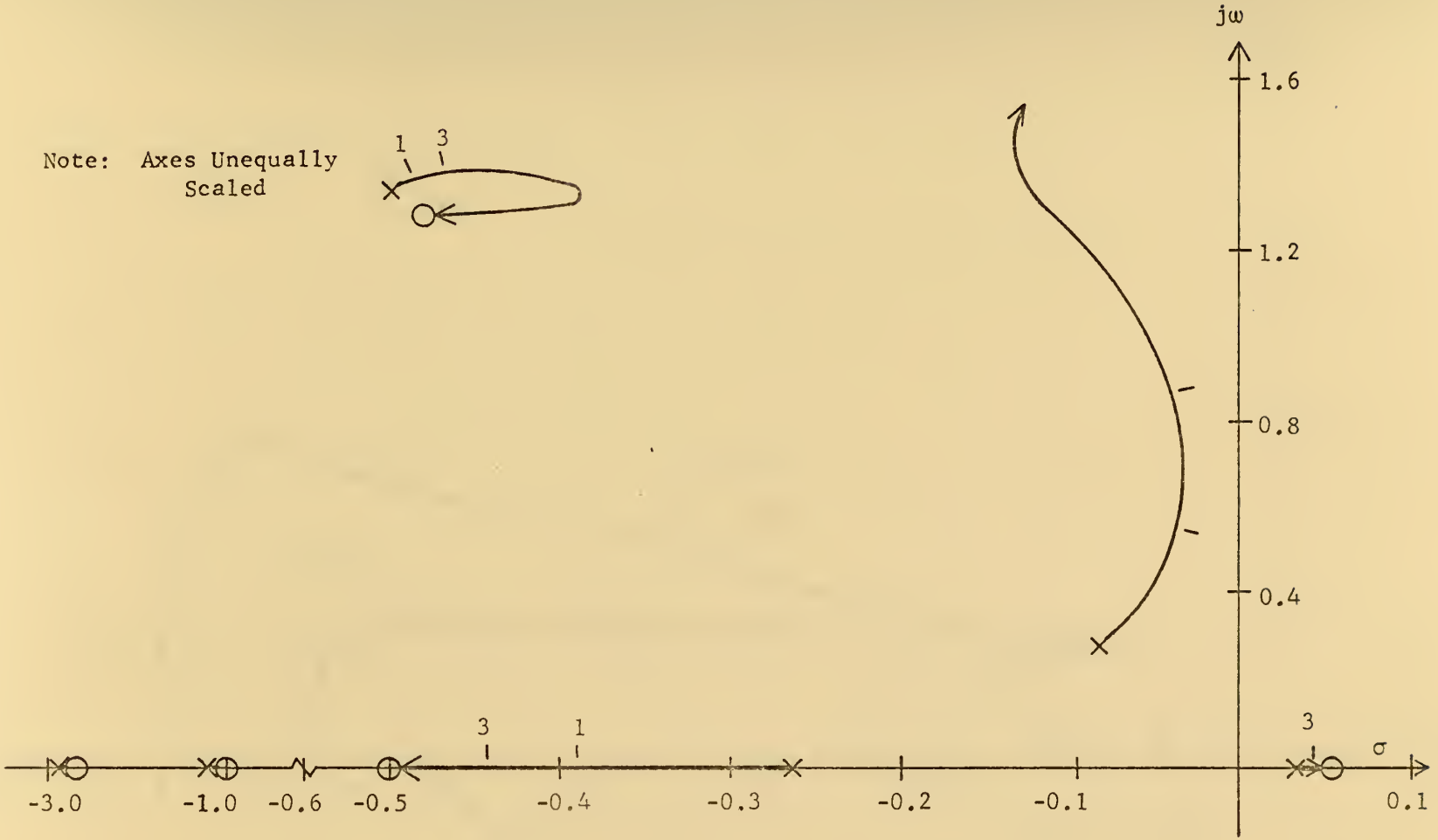

FIGURE 13. LOCI OF ZEROES OF Δ''' FOR K_u VARIATION; $K_p = 0.5$

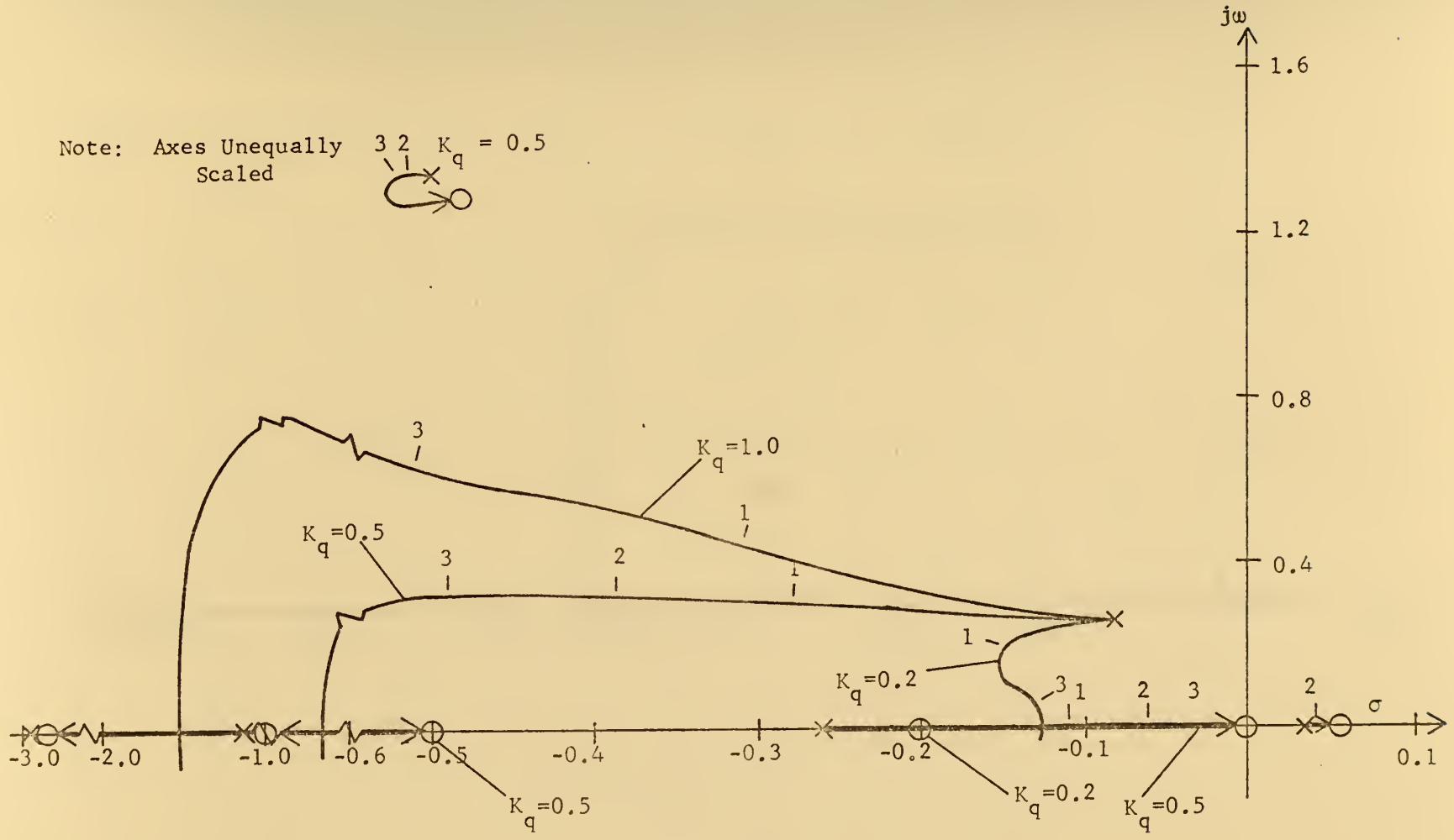

FIGURE 14. LOCI OF ZEROES OF Δ''' FOR K_u VARIATION; K_q=0.2,0.5,1.0

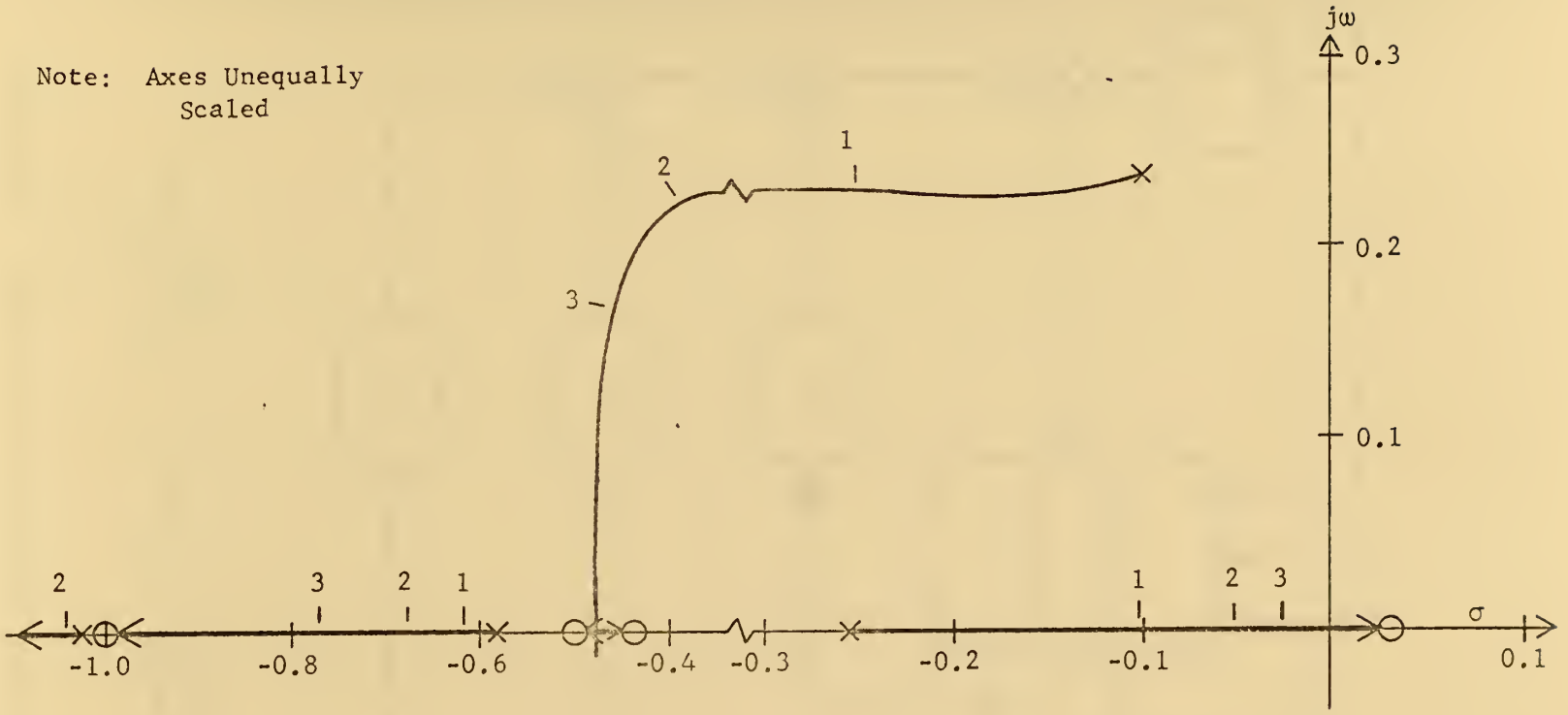

FIGURE 15. LOCI OF ZEROES OF $N^{w}_{\delta_e}]$ FOR K_u^* VARIATION; K_q=0.5

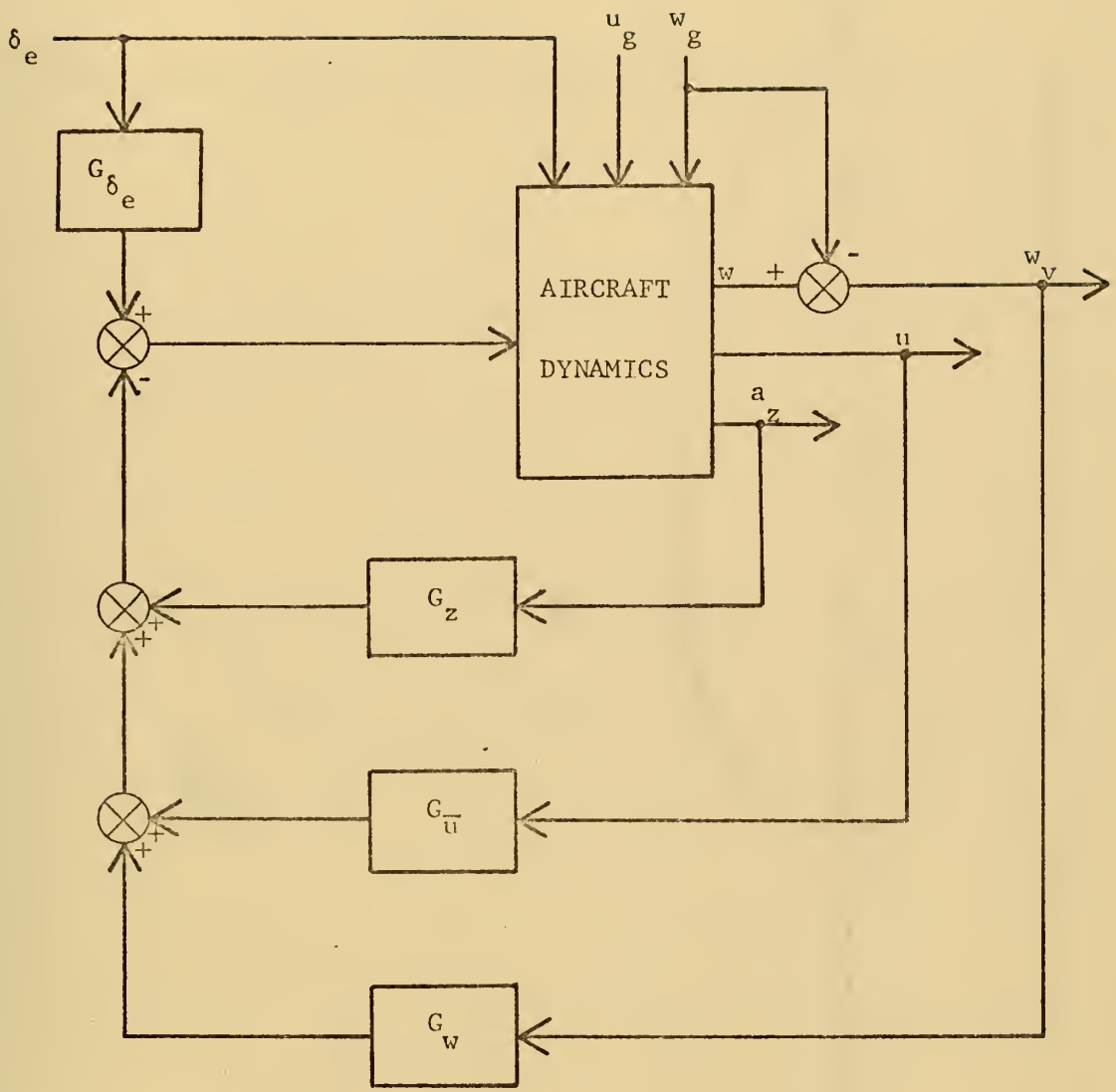

$$G_{\overline{u}} = \frac{350.7}{T_e(s+1/T_e)} \cdot K_u^{\cdot} (s+K_q) = \frac{701.4(s+0.5)}{T_e(s+1/T_e)}$$

FIGURE 16. REVISED APCS EQUIVALENT BLOCK DIAGRAM

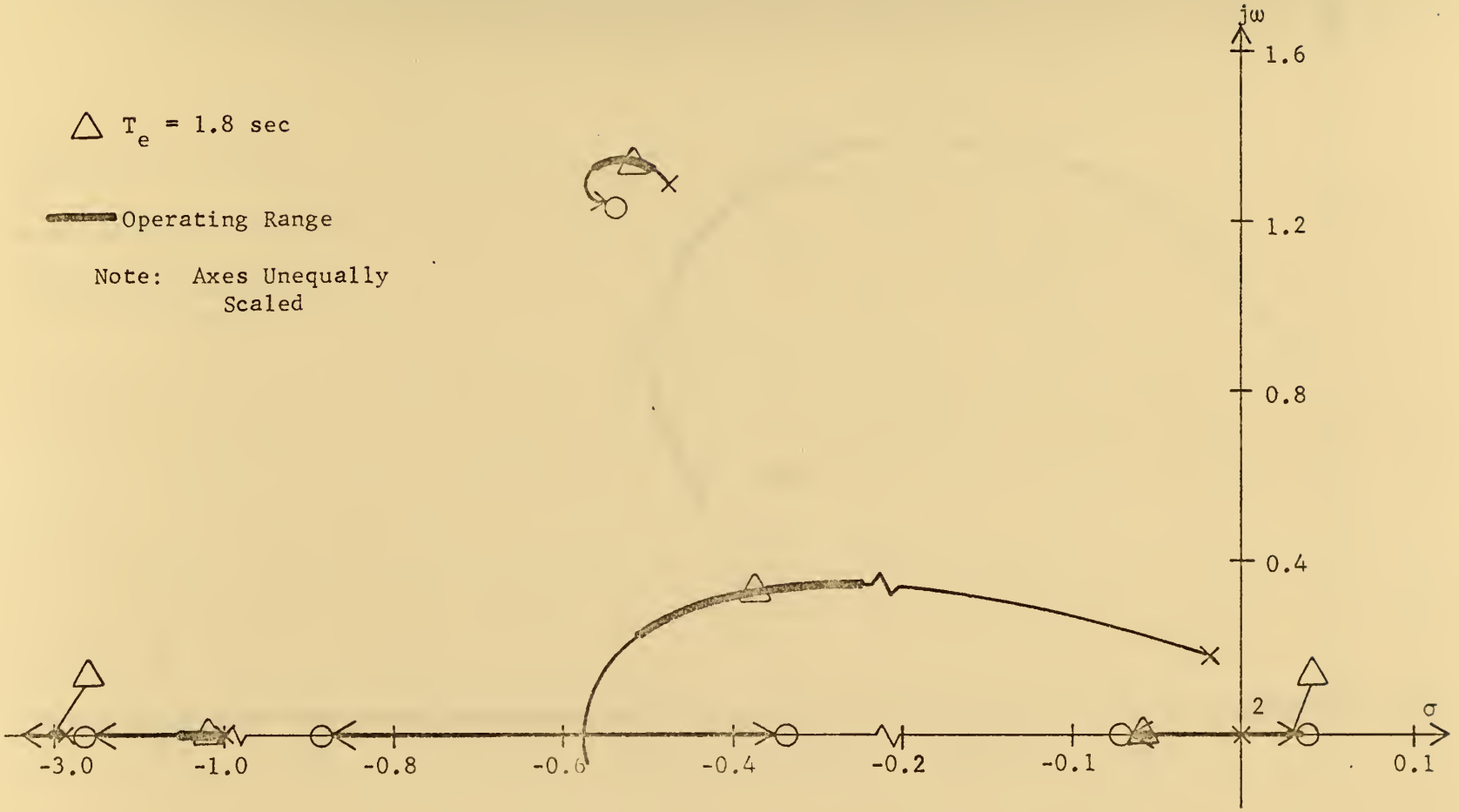

FIGURE 17. LOCI OF ZEROES Δ''' FOR $1/T_e$ VARIATION; REVISED CONFIGURATION

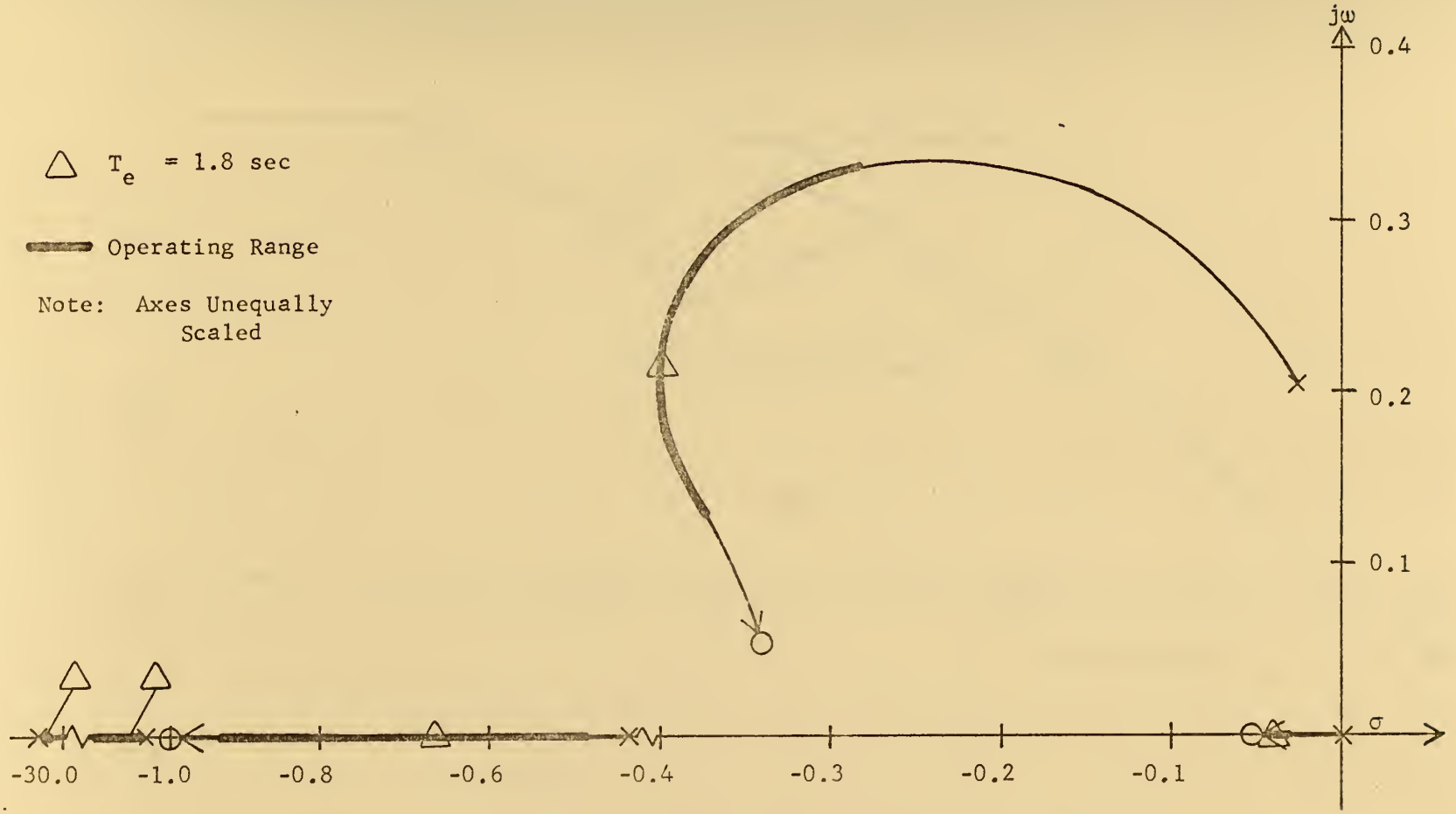

FIGURE 18. LOCI OF ZEROES OF $N^w_{\delta_e}]_{rev}$ FOR $1/T_e$ VARIATION; REVISED CONFIGURATION

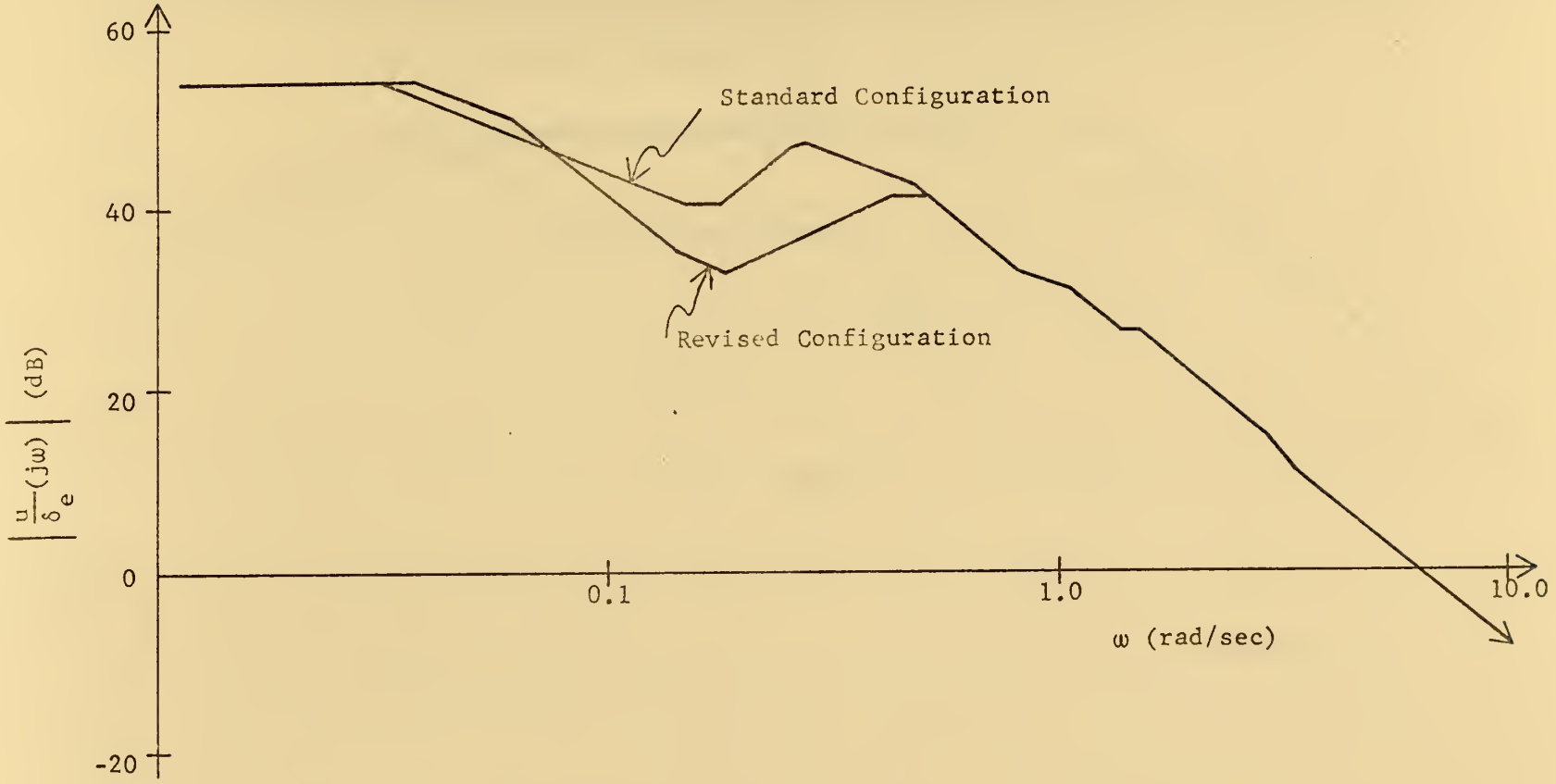

FIGURE 19. AIRSPEED REPSONSE TO ELEVATOR, BODE PLOT

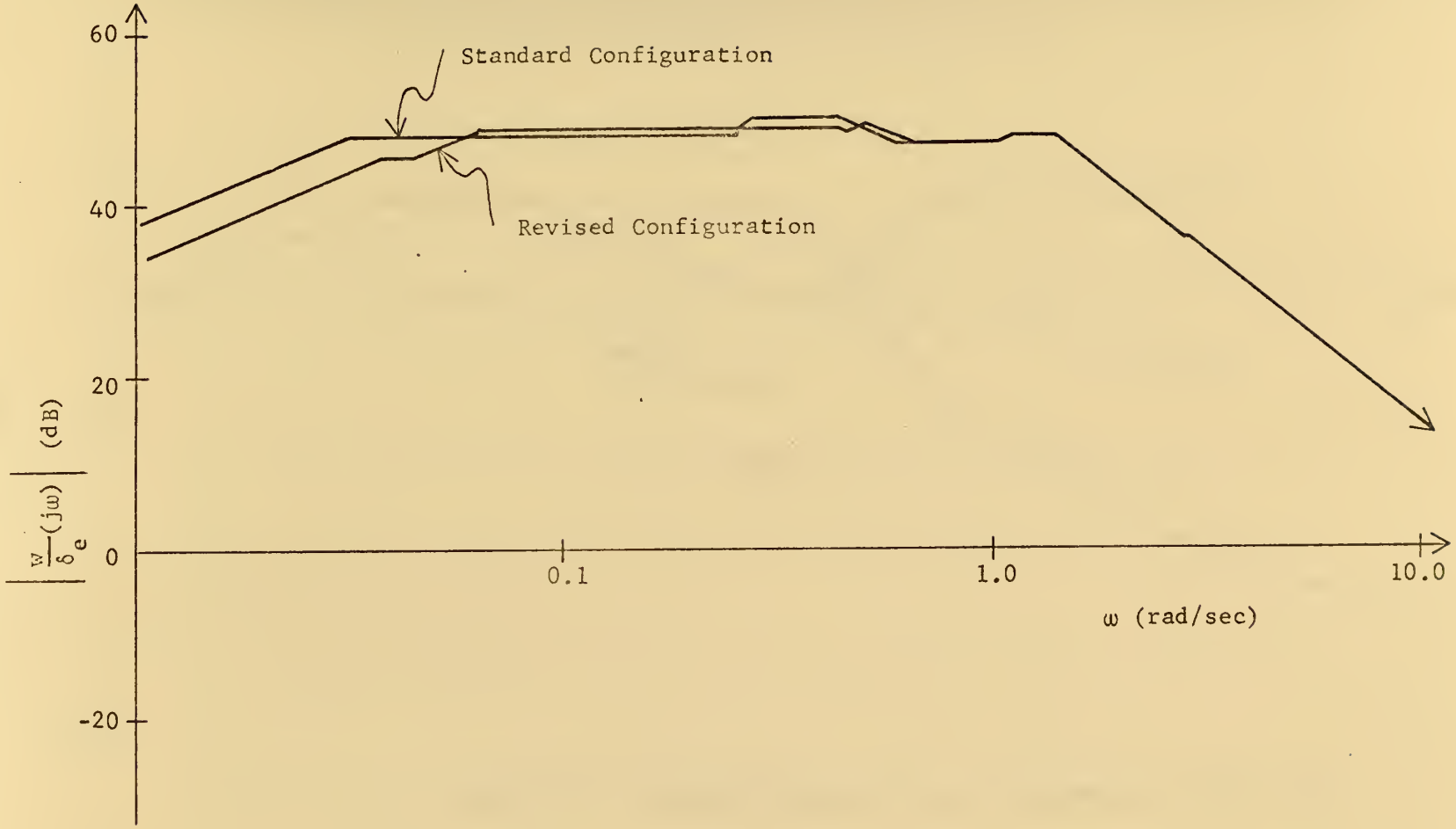

FIGURE 20. ANGLE OF ATTACK RESPONSE TO ELEVATOR, BODE PLOT

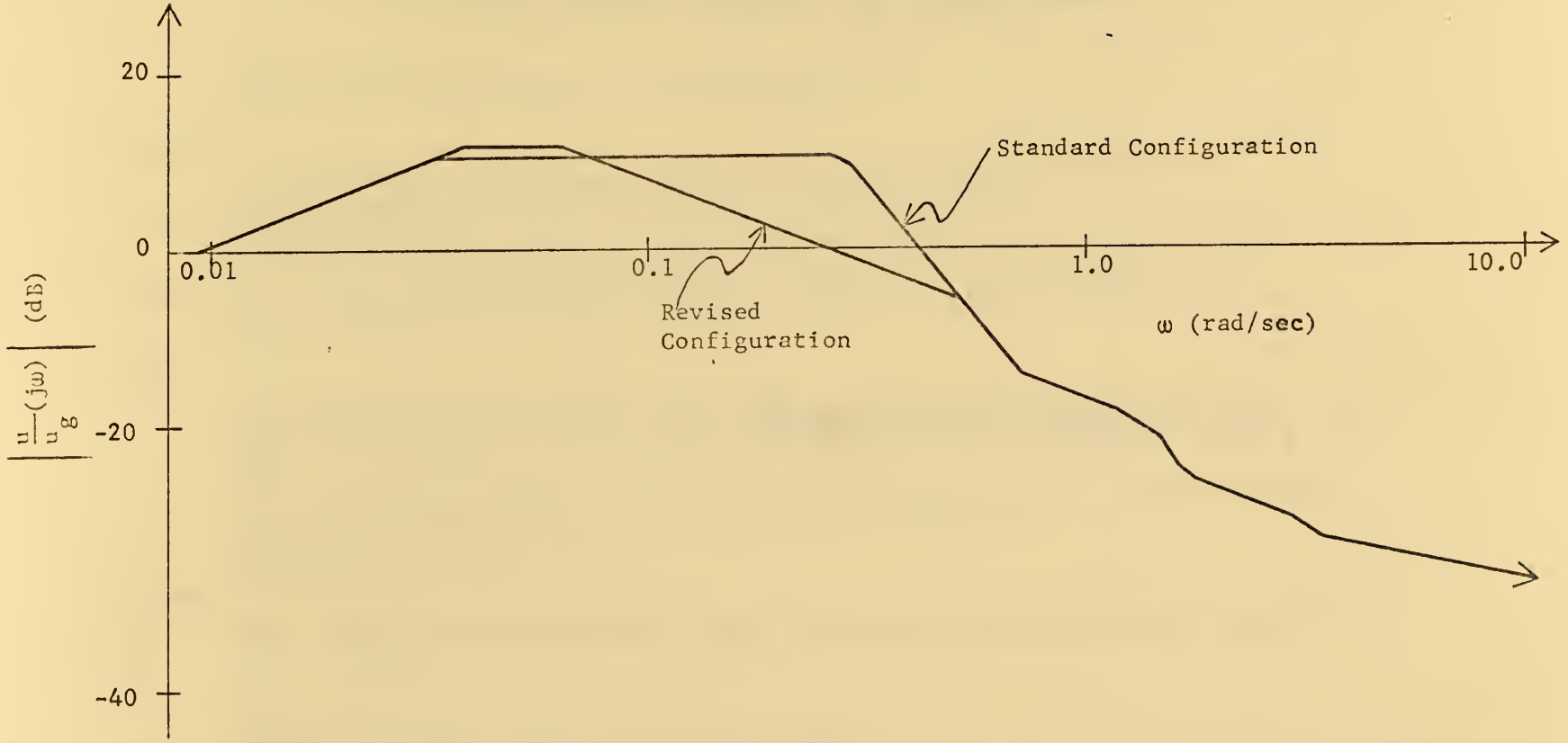

FIGURE 21. AIRSPEED RESPONSE TO LONGITUDINAL GUST, BODE PLOT

APPENDIX A

CSMP COMPUTER PROGRAM AND SAMPLE OUTPUT

```
/       DIMENSION A(4,4),B(4,4),C(3,4),D(3,4)
        FIXED I,J
INITIAL
NOSORT
        READ(5,100) ((A(I,J),J=1,4),I=1,4),((B(I,J),J=1,4),I=1,4),      ...
        ((C(I,J),J=1,4),I=1,3),((D(I,J),J=1,4),I=1,3)
  100   FORMAT(4F10.6)
        WRITE(6,1000) ((A(I,J),J=1,4),(B(I,J),J=1,4),I=1,4),((C(I,J),   ...
        J=1,4),(D(I,J),J=1,4),I=1,3)
 1000   FORMAT('0',T35,'A-MATRIX',T99,'B-MATRIX'//4(T06,4F15.6,T71,
       $4F15.6/)//T35,'C-MATRIX',T99,'D-MATRIX'//3(T06,4F15.6,T71,
       $4F15.6/)//)
SORT


        FUNCTION TECURV=-2100.0,4.0,-1800.0,2.5,-1500.0,2.25,-1200.0,    ...
        2.18.-800.0,2.13,-400.0,2.08,-200.0,2.03,0.0,1.85,200.0,1.55,    ...
        400.0,1.27,600.0,1.15,800.0,1.1,1200.0,1.05,2000.0,1.0,3000.0,   ...
        1.0
        PARAM A0=0.0242,A1=0.369,B0=66.489,B1=43.989,B2=9.7996,K=0.5923
        INCON X10=0.0,X20=0.0,X30=0.0,X40=0.0,ZE0=0.0
        CONSTANT KP=0.5,KUDOT=2.0
        WGUST=0.0
DYNAMIC
*
*       APCS INCLUDES PROPORTIONSL PLUS DERIVATIVE LONGITUDINAL VELOCITY
*
*       GUST INPUT
*
        RAND=385.0*(RNDGEN(3)-0.5)
        UGUST=CMPXPL(0.0,0.0,0.707,1.0,RAND)
        UG=UGUST**2
        UGMSV=INTGRL(0.0,UG)
*
*       AIRCRAFT EQUATIONS OF MOTION
*
        XTEMP1=A(1,1)*X1+A(1,2)*X2+A(1,3)*X3+A(1,4)*X4+B(1,1)*ELEV       ...
        +B(1,2)*THRUST+B(1,3)*UGUST+B(1,4)*WGUST
        X1=INTGRL(X10,XTEMP1)
        XTEMP2=A(2,1)*X1+A(2,2)*X2+A(2,3)*X3+A(2,4)*X4+B(2,1)*ELEV       ...
        +B(2,2)*THRUST+B(2,3)*UGUST+B(2,4)*WGUST
```

```
      X2=INTGRL(X20,XTEMP2)
      X3=INTGRL(X30,X4)
      XTEMP4=A(4,1)*X1+A(4,2)*X2+A(4,3)*X3+A(4,4)*X4+B(4,1)*ELEV      ...
     +B(4,2)*THRUST+B(4,3)*UGUST+B(4,4)*WGUST
      X4=INTGRL(X40,XTEMP4)
      HDOT   =C(1,1)*X1+C(1,2)*X2+C(1,3)*X3+C(1,4)*X4
      AZ     =C(2,1)*X1+C(2,2)*X2+C(2,3)*X3+C(2,4)*X4+D(2,1)*ELEV      ...
     +D(2,2)*THRUST+D(2,3)*UGUST+D(2,4)*WGUST
      AZPRIM=C(3,1)*X1+C(3,2)*X2+C(3,3)*X3+C(3,4)*X4+D(3,1)*ELEV      ...
     +D(3,2)*THRUST+D(3,3)*UGUST+D(3,4)*WGUST+AZ
*
**    APCS EQUATIONS
*
      ALPHAV=0.3651*(X2-WGUST)
      ALPHAI=0.55*INTGRL(0.0,ALPHAV)
      ALPHA=INTGRL(0.0,(2.6*ALPHAV-ALPHA)/0.35)
      W1DOT=-0.435*W1+ELEV
      W1=INTGRL(0.0,W1DOT)
      ELEVP=143.2*W1DOT
      NZP=1.0-0.03109*AZPRIM
      NZACC=REALPL(1.0,1.0,NZP)
      NZBAR=30.0*(1.0-NZACC)
      TE=AFGEN(TECURV,THRUST)
      PLA=NZBAR+ALPHA+ALPHAI-ELEVP-KUDOT*(XTEMP1+KP*X1)
      THRUST=INTGRL(0.0,(350.7*PLA-THRUST)/TE)
*
**    ACLS EQUATIONS
*
      ZE=INTGRL(ZE0,-HDOT)
      ZI=K*INTGRL(0.0,ZE)
      Y1=INTGRL(0.0,Y2)
      Y2=INTGRL(0.0,Y3)
      Y3DOT=-B0*Y1-B1*Y2-B2*Y3+ZI
      Y3=INTGRL(0.0,Y3DOT)
      THETAC=Y3+A1*Y2+A0*Y1
*
**    AFCS EQUATIONS
*
      AZSTAR=REALPL(0.0,0.55,AZ)
      ELEV=1.9*(X3-THETAC)+X4-0.00163*AZSTAR
*
**    VERTICAL AND HORIZONTAL VELOCITY ERROR
*
      ERR1=X1**2
      ERR2=X2**2
      ERRCUM=INTGRL(0.0,ERR1+ERR2)
*
      TIMER FINTIM=30.0,DELT=0.0500,OUTDEL=0.10,PRDEL=0.5
```

```
      METHOD RKSFX
      TITLE  A-7E AIRCRAFT WITH APC/AFCS/ACL CLOSURES
      PRINT ZE,THETAC,ELEV,ELEVP,NZBAR,PLA,THRUST,ERRCUM
      PREPARE X1,X2,ZE,THRUST,UGUST
TERMINAL
      ERRRMS=SQRT(ERRCUM/30.0)
      WRITE(6,2000) ERRRMS
 2000 FORMAT('0',T10,'RMS VELOCITY ERROR=',F10.4///)
      UGRMS=SQRT(UGMSV/30.0)
      WRITE(6,3000) UGRMS
 3000 FORMAT('0',T10,'RMS GUST LEVEL:',2F15.4//)
END
DATA
-0.05453   0.06433   -32.16     0.0
-0.2870    -0.5289   0.0        218.0
0.0        0.0       0.0        1.0
-0.000082 -0.007811  0.0        -0.3905
0.7328     0.001317  0.05453    -0.06433
-14.714    -0.00025  0.28695    0.52887
0.0        0.0       0.0        0.0
-2.1846    0.000004  0.000082   0.007811
0.0        -1.0      218.0      0.0
-0.28695  -0.52887   0.0        0.0
0.00055    0.052334  0.0        2.61635
0.0        0.0       0.0        0.0
-14.714    -0.00025  0.28695    0.52887
14.6368    -0.000027 -0.00055   -0.052334
ENDDATA
STOP
ENDJOB
```

```
C      OFFLINE PLOTTING ROUTINE

       DIMENSION XOUT(6),X(900),U(900),V(900),W(900),Y(900),Z(900)
       REAL * 8 LABEL/8H          /,ITITLE(12)
       DATA ENDS/'ENDS'/
       DOUBLE PRECISION WORD

C      KGRAPH IS NO OF OUTPUT VARIABLES

       KGRAPH=6

C      READ CONSTANTS FOR DRAW

       READ(5,100) NOPLOT
     5 READ(5,100) NOCUR
   100 FORMAT(I2)
       READ(5,200) (ITITLE(I),I=1,12)
   200 FORMAT(6A8)
       READ(5,300) XSCL,YSCL,IUP,IRITE,MODEX,MODEY,IW,IHI,IGR
   300 FORMAT(9I5)
       IF(NOCUR-1) 55,10,15
    10 MODCUR=0
       GO TO 20
    15 MODCUR=1

C      READ DATA SET OF POINTS PRODUCED BY CSMP

    20 CONTINUE

C      READ 10 INTRODUCTORY RECORDS

       DO 25 I=1,10
    25 READ (15) WORD
       NUMPTS=0

C      READ POINTS

    30 READ (15) (XOUT(I),I=1,KGRAPH)
       IF(XOUT(1)-ENDS) 35,40,35
    35 NUMPTS=NUMPTS+1
       X(NUMPTS)=XOUT(1)
       U(NUMPTS)=XOUT(2)
       V(NUMPTS)=XOUT(3)
       W(NUMPTS)=XOUT(4)
       Y(NUMPTS)=XOUT(5)
```

```
      Z(NUMPTS)=XOUT(6)
      GO TO 30
   40 CONTINUE

C     CALL DRAW

      CALL DRAW(NUMPTS,X,U,MODCUR,0,LABEL,ITITLE,XSCL,YSCL,IUP,IRITE,
     CMODEX,MODEY,IW,IHI,IGR,LAST)
      READ(5,200) (ITITLE(I),I=1,12)
      CALL DRAW(NUMPTS,X,V,MODCUR,0,LABEL,ITITLE,XSCL,YSCL,IUP,IRITE,
     CMODEX,MODEY,IW,IHI,IGR,LAST)
      READ(5,200) (ITITLE(I),I=1,12)
      CALL DRAW(NUMPTS,X,W,MODCUR,0,LABEL,ITITLE,XSCL,YSCL,IUP,IRITE,
     CMODEX,MODEY,IW,IHI,IGR,LAST)
      READ(5,200) (ITITLE(I),I=1,12)
      CALL DRAW(NUMPTS,X,Y,MODCUR,0,LABEL,ITITLE,XSCL,YSCL,IUP,IRITE,
     CMODEX,MODEY,IW,IHI,IGR,LAST)
      READ(5,200) (ITITLE(I),I=1,12)
      CALL DRAW(NUMPTS,X,Z,MODCUR,0,LABEL,ITITLE,XSCL,YSCL,IUP,IRITE,
     CMODEX,MODEY,IW,IHI,IGR,LAST)
      NOCUR=NOCUR-1
      IF(NOCUR-1) 55,45,50
   45 MODCUR=3
      READ (15) WORD
      GO TO 20
   50 MODCUR=2
      READ (15) WORD
      GO TO 20
   55 NOPLOT=NOPLOT-1
      IF(NOPLOT) 60,60,5
   60 STOP
      END

C     DATA CARDS

 1
 1
U VS TIME   U GUST INPUT
APCS INCL U AND DERIV U INPUTS
    0    0    0    0    0    0    8    4    1
W VS TIME   U GUST INPUT
APCS INCL U AND DERIV U INPUTS
ZE VS TIME   U GUST INPUT
APCS INCL U AND DERIV U INPUTS
THRUST VS TIME U GUST INPUT
APCS INCL U AND DERIV U INPUTS
UGUST VS TIME
APCS INCL U AND DERIV U INPUTS
```

```
                    *** CSMP/360 SIMULATION DATA ***
      FUNCTION TECURV=-2100.0,4.0,-1800.0,2.5,-1500.0,2.25,-1200.0,  ...
      2.18,-800.0,2.13,-400.0,2.08,-200.0,2.03,0.0,1.85,200.0,1.55,  ...
      400.0,1.27,600.0,1.15,800.0,1.1,1200.0,1.05,2000.0,1.0,3000.0, ...
      1.0
      PARAM A0=0.0242,A1=0.369,B0=66.489,B1=43.989,B2=9.7996,K=0.5923
      INCON X10=0.0,X20=0.0,X30=0.0,X40=0.0,ZE0=0.0
      CONSTANT KP=0.5,KUDOT=2.0
      TIMER FINTIM=30.0,DELT=0.0500,OUTDEL=0.10,PRDEL=0.5
      METHOD RKSFX
      TITLE  A-7E AIRCRAFT WITH APC/AFCS/ACL CLOSURES
      PRINT ZE,THETAC,ELEV,ELEVP,NZBAR,PLA,THRUST,ERRCUM
      PREPARE X1,X2,ZE,THRUST,UGUST
END

TIMER VARIABLES
 DELT  = 5.0000E-02
 DELMIN= 3.0000E-06
 FINTIM= 3.0000E 01
 PRDEL = 5.0000E-01
 OUTDEL= 1.0000E-01
```

A-MATRIX

-0.054530	0.064330	-32.159988	0.0	0.732800
-0.287000	-0.528900	0.0	218.000000	-14.714000
0.0	0.0	0.0	1.000000	0.0
-0.000082	-0.007811	0.0	-0.390500	-2.184600

B-MATRIX

0.001317	0.054530	-0.064330	
-0.000250	0.286950	0.528870	
0.0	0.0	0.0	
0.000004	0.000082	0.007811	

C-MATRIX

0.0	-1.000000	218.000000	0.0	0.0
-0.286950	-0.528870	0.0	0.0	-14.714000
0.000550	0.052334	0.0	2.616349	14.636800

D-MATRIX

0.0	0.0	0.0	
-0.000250	0.286950	0.528870	
-0.000027	-0.000550	-0.052334	

RB A-7E AIRCRAFT WITH APC/AFCS/ACL CLOSURES RKSFX INTEGRATION

TIME	ZE	THETAC	ELEV	ELEVP	NZBAR	PLA	THRUST	ERRCUM
0.0	0.0	0.0	0.0	0.0	0.0	0.0	0.0	0.0
5.0000E-01	-5.3992E-02	-1.7875E-04	1.0093E-03	1.3528E-01	-2.4284E-01	-1.3176E-03	9.5747E 00	1.1037E-02
1.0000E 00	-3.0122E-01	-2.2438E-03	4.0226E-03	4.9827E-01	-3.5391E-01	-7.9524E-01	-3.0614E 01	1.4822E-01
1.5000E 00	-6.3296E-01	-5.3608E-03	5.3997E-03	5.6963E-01	-2.2699E-01	-1.0152E 00	-1.8830E 01	4.7459E-01
2.0000E 00	-9.0421E-01	-7.1930E-03	3.7099E-03	2.3584E-01	6.4353E-02	-6.4892E-01	-1.4500E 02	9.9655E-01
2.5000E 00	-1.0268E 00	-6.7948E-03	1.3774E-03	-1.0871E-01	2.5422E-01	-3.1659E-01	-1.4956E 02	1.6520E 00
3.0000E 00	-1.0215E 00	-5.0947E-03	6.2312E-04	-1.8046E-01	2.7504E-01	-2.7179E-01	-1.3566E 02	2.2953E 00
3.5000E 00	-9.5711E-01	-3.4750E-03	1.3164E-03	-5.3990E-02	1.7449E-01	-2.3408E-01	-1.2278E 02	2.7864E 00
4.0000E 00	-9.3826E-01	-2.9555E-03	2.9587E-03	1.6907E-01	-1.1209E-01	-9.5770E-02	-1.0754E 02	3.2054E 00
4.5000E 00	-1.1927E 00	-4.8147E-03	7.0522E-03	6.7217E-01	-6.0122E-01	-8.7321E-01	-1.1601E 02	4.0538E 00
5.0000E 00	-1.7702E 00	-1.0464E-02	1.1664E-02	1.1277E 00	-6.3758E-01	-1.9215E 00	-2.0517E 02	6.0253E 00
5.5000E 00	-2.4159E 00	-1.6184E-02	1.1725E-02	9.0366E-01	-3.1211E-01	-1.7624E 00	-3.0604E 02	9.4428E 00
6.0000E 00	-2.9679E 00	-1.9054E-02	9.0199E-03	3.7708E-01	1.0380E-01	-1.7192E 00	-3.7198E 02	1.4807E 01
6.5000E 00	-3.2174E 00	-1.8579E-02	5.8206E-03	-1.0942E-01	5.7481E-01	-1.2548E 00	-4.0549E 02	2.1031E 01
7.0000E 00	-3.0964E 00	-1.4674E-02	2.4061E-03	-5.2692E-01	8.8669E-01	-6.4616E-01	-3.9309E 02	2.6478E 01
7.5000E 00	-2.6140E 00	-8.6154E-03	-6.9344E-04	-8.2204E-01	9.7843E-01	1.6203E-01	-3.2717E 02	3.0141E 01
8.0000E 00	-1.8547E 00	-1.8899E-03	-3.6200E-03	-1.0390E 00	9.6906E-01	9.0139E-01	-2.1722E 02	3.2532E 01
8.5000E 00	-8.7718E-01	4.8954E-03	-6.6806E-03	-1.2281E 00	7.1942E-01	2.0193E 00	-4.8619E 01	3.4993E 01
9.0000E 00	5.1763E-02	1.0110E-02	-7.1405E-03	-1.0377E 00	1.7577E-01	2.0400E 00	1.4718E 02	3.8367E 01
9.5000E 00	7.4341E-01	1.1540E-02	-4.7121E-03	-5.1928E-01	-3.1534E-01	1.5509E 00	2.8155E 02	4.2348E 01
1.0000E 01	1.1117E 00	9.7079E-03	-2.0117E-03	-9.7965E-02	-6.3312E-01	9.1601E-01	3.2153E 02	4.5986E 01
1.0500E 01	1.1792E 00	5.9961E-03	-3.7407E-04	1.5737E-01	-8.1573E-01	5.0165E-01	2.9675E 02	4.8495E 01
1.1000E 01	9.0769E-01	1.1026E-03	2.6689E-03	5.3678E-01	-9.8574E-01	-5.3067E-01	2.1436E 02	4.9789E 01
1.1500E 01	3.8648E-01	-4.9098E-03	5.7660E-03	8.1819E-01	-7.9187E-01	-1.3174E 00	6.1274E 01	5.0965E 01
1.2000E 01	-2.8652E-01	-1.0007E-02	8.0831E-03	9.5836E-01	-8.0054E-01	-1.7425E 00	-7.4263E 01	5.3351E 01
1.2500E 01	-1.1809E 00	-1.6547E-02	1.2225E-02	1.0374E 00	-7.3485E-01	-2.8160E 00	-2.3736E 02	5.8795E 01
1.3000E 01	-2.1682E 00	-2.1403E-02	1.5476E-02	1.4640E 00	-4.7450E-01	-3.2724E 00	-4.2092E 02	6.7944E 01
1.3500E 01	-3.1452E 00	-2.5884E-02	1.6476E-02	1.2041E 00	-2.3440E-01	-3.2573E 00	-5.7375E 02	8.1292E 01
1.4000E 01	-4.0867E 00	-2.9161E-02	1.7195E-02	1.1404E 00	2.0896E-02	-3.4725E 00	-6.9768E 02	9.9351E 01
1.4500E 01	-4.7395E 00	-3.0727E-02	1.5605E-02	7.0568E-01	6.0651E-01	-3.0601E 00	-7.9800E 02	1.1991E 02
1.5000E 01	-4.9064E 00	-2.7917E-02	9.6233E-03	-2.1279E-01	1.2147E 00	-1.7180E 00	-8.0676E 02	1.3932E 02
1.5500E 01	-4.4537E 00	-2.0274E-02	1.9023E-03	-1.1656E 00	1.6612E 00	-2.4192E-01	-7.0338E 02	1.5527E 02
1.6000E 01	-3.3119E 00	-8.8404E-03	-6.2463E-03	-2.0010E 00	2.0105E 00	1.6245E 00	-5.0524E 02	1.6687E 02
1.6500E 01	-1.5765E 00	5.4918E-03	-1.4067E-02	-2.5979E 00	1.8099E 00	3.4525E 00	-1.9494E 02	1.7698E 02
1.7000E 01	4.5339E-01	1.9024E-02	-1.8525E-02	-2.6571E 00	1.3570E 00	4.2615E 00	1.8411E 02	1.9053E 02
1.7500E 01	2.6068E 00	2.9983E-02	-2.1964E-02	-2.5818E 00	9.1076E-01	4.7347E 00	6.3290E 02	2.1190E 02
1.8000E 01	4.7133E 00	3.8714E-02	-2.5252E-02	-2.4975E 00	3.1159E-01	4.9853E 00	1.0395E 03	2.4224E 02
1.8500E 01	6.6093E 00	4.4392E-02	-2.7124E-02	-2.2492E 00	-7.2126E-02	4.6149E 00	1.2834E 03	2.7924E 02
1.9000E 01	8.3595E 00	4.8476E-02	-2.9715E-02	-2.1429E 00	-2.9895E-01	5.0658E 00	1.4373E 03	3.2244E 02
1.9500E 01	9.7000E 00	5.1259E-02	-2.8305E-02	-1.5254E 00	-1.2140E 00	4.4571E 00	1.5541E 03	3.6524E 02
2.0000E 01	1.0174E 01	4.7132E-02	-1.9005E-02	-1.0386E-01	-2.1181E 00	2.0878E 00	1.3948E 03	3.9891E 02
2.0500E 01	9.7731E 00	3.5796E-02	-7.7541E-03	1.4016E 00	-2.3021E 00	3.0973E-01	1.0058E 03	4.2209E 02
2.1000E 01	8.8295E 00	2.3083E-02	-4.3493E-03	1.5512E 00	-1.8773E 00	-7.3944E-02	6.4376E 02	4.3565E 02
2.1500E 01	7.6296E 00	1.3263E-02	-3.9508E-03	1.3015E 00	-1.3740E 00	-4.7756E-01	3.9481E 02	4.4212E 02
2.2000E 01	6.3040E 00	6.1741E-03	-1.1675E-03	1.4116E 00	-9.7246E-01	-1.4251E 00	1.8201E 02	4.4540E 02
2.2500E 01	4.9553E 00	6.8485E-04	2.8568E-03	1.4515E 00	-5.2302E-01	-2.2177E 00	-3.0911E 01	4.4849E 02
2.3000E 01	3.7178E 00	-2.9080E-03	4.7392E-03	1.5620E 00	-8.1196E-02	-2.1662E 00	-2.0278E 02	4.5195E 02
2.3500E 01	2.6407E 00	-4.5010E-03	4.9696E-03	1.2360E 00	1.4950E-01	-1.7712E 00	-3.0117E 02	4.5541E 02
2.4000E 01	1.7445E 00	-5.1185E-03	4.7962E-03	1.0112E 00	3.0457E-01	-1.2009E 00	-3.4997E 02	4.5845E 02
2.4500E 01	1.0160E 00	-4.7886E-03	4.4312E-03	7.6820E-01	3.8683E-01	-6.6790E-01	-3.4310E 02	4.6087E 02
2.5000E 01	3.1950E-01	-4.9666E-03	3.9691E-03	8.2220E-01	1.3398E-01	-6.1651E-01	-3.1226E 02	4.6294E 02
2.5500E 01	-4.8360E-01	-7.3312E-03	3.8349E-03	1.3965E 00	-9.6645E-02	-1.0999E 00	-3.1046E 02	4.6516E 02
2.6000E 01	-1.3719E 00	-1.1433E-02	1.1460E-02	1.1484E 00	-3.8767E-02	-1.4687E 00	-3.4622E 02	4.6791E 02
2.6500E 01	-2.1602E 00	-1.4744E-02	1.3126E-02	7.4417E-01	2.6490E-01	-1.2562E 00	-3.7648E 02	4.7126E 02
2.7000E 01	-2.7061E 00	-1.5227E-02	6.5913E-03	1.4168E-01	6.2061E-01	-7.6121E-01	-3.6953E 02	4.7490E 02
2.7500E 01	-2.8515E 00	-1.2519E-02	2.1650E-03	-4.5098E-01	1.1031E 00	-3.0522E-01	-3.3452E 02	4.7880E 02
2.8000E 01	-2.4260E 00	-5.8136E-03	-4.2006E-03	-1.1925E 00	1.4866E 00	1.1244E 00	-2.3347E 02	4.7875E 02
2.8500E 01	-1.5320E 00	4.0314E-03	-9.6564E-03	-1.6534E 00	1.3499E 00	2.2493E 00	-3.9388E 01	4.7694E 02
2.9000E 01	-4.1940E-01	1.3106E-02	-1.1400E-02	-1.5471E 00	9.4230E-01	2.7206E 00	1.9290E 02	4.8059E 02
2.9500E 01	6.5426E-01	1.9218E-02	-1.0832E-02	-1.1683E 00	3.2426E-01	2.6192E 00	4.2716E 02	4.8531E 02
3.0000E 01	1.5604E 00	2.1578E-02	-1.0606E-02	-9.1679E-01	7.7714E-02	2.3547E 00	5.6931E 02	4.9332E 02

PROBLEM DURATION 0.0 TO 3.0000E 01

VARIABLE	MINIMUM	TIME	MAXIMUM	TIME
X1	-4.4800E 00	1.5750E 01	2.4423E 00	2.1600E 01
X2	-5.3625E 00	1.4100E 01	9.4773E 00	1.9000E 01
ZF	-4.9204E 00	1.4900E 01	1.0174E 01	2.0000E 01
THRUST	-8.1744E 02	1.4800E 01	1.5541E 03	1.9500E 01
UGUST	-1.1338E 01	1.3700E 01	1.4372E 01	1.8650E 01

RMS VELOCITY ERROR= 4.0551

RMS GUST LEVEL: 5.0217

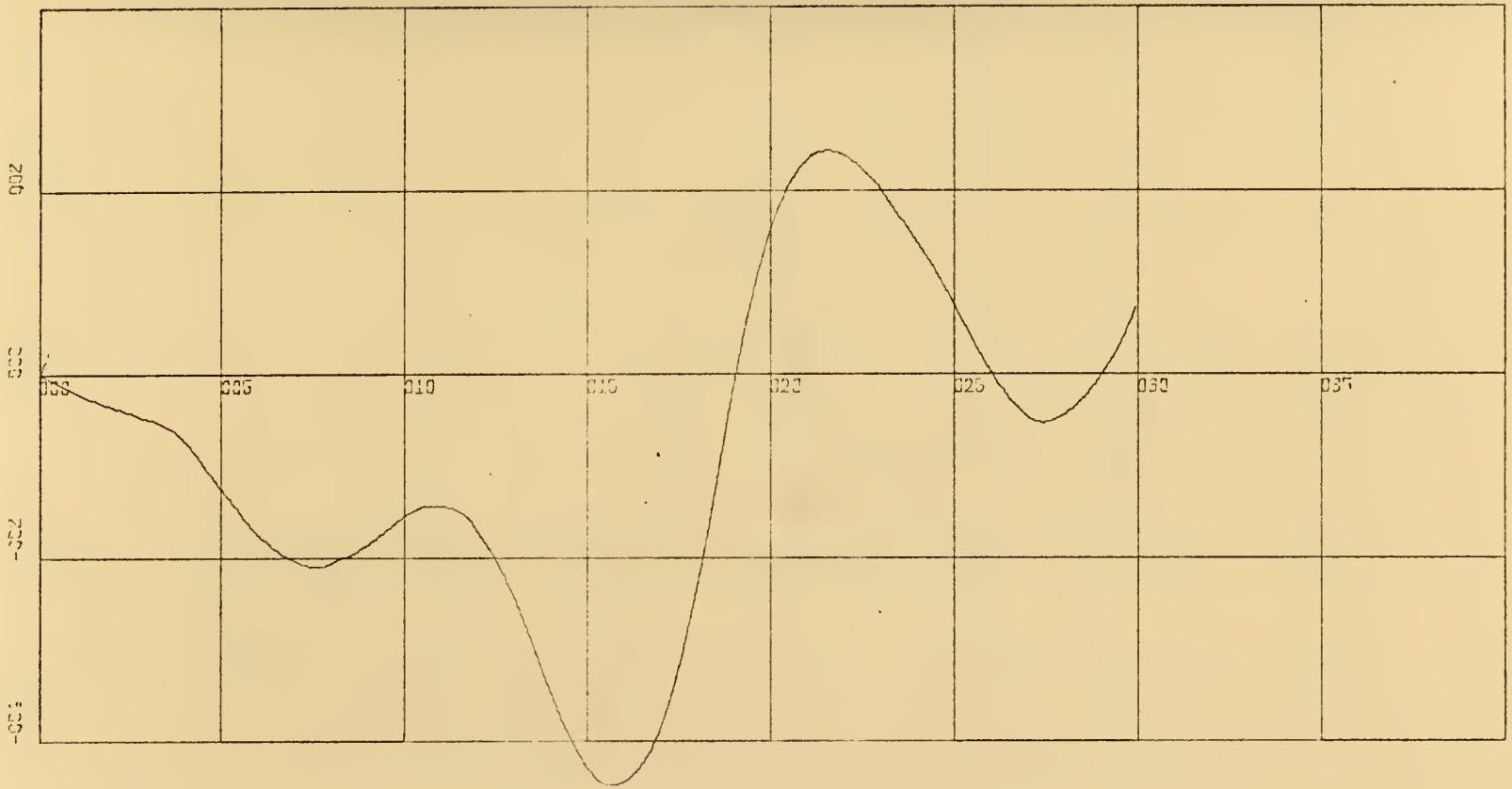

X-SCALE=5.00E+00 UNITS INCH.
Y-SCALE=2.00E+00 UNITS INCH.
U VS TIME U GUST INPUT
APCS INCL U AND DERIV U INPUTS

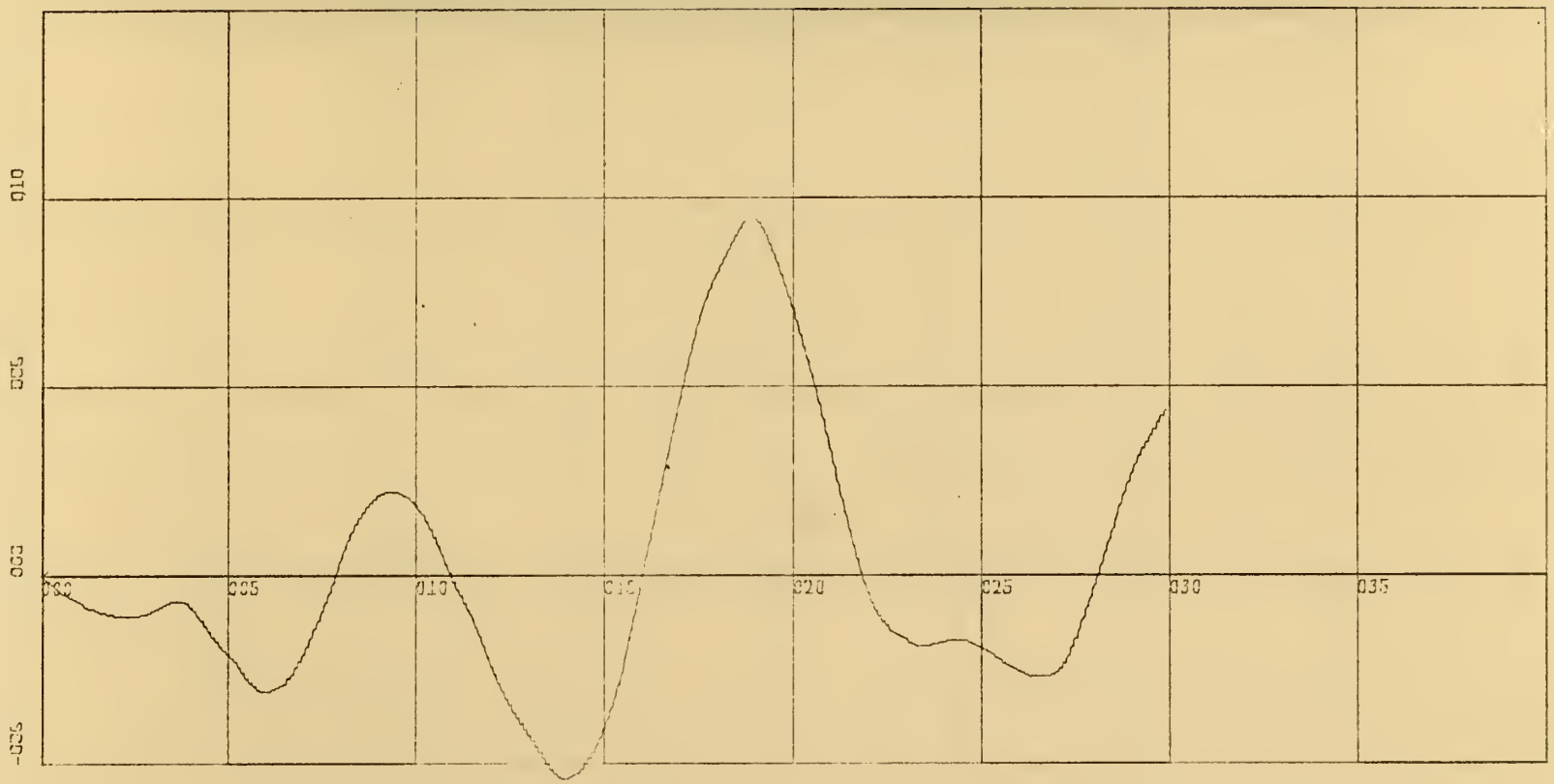

X-SCALE=5.00E+00 UNITS INCH.
Y-SCALE=5.00E+00 UNITS INCH.
W VS TIME U GUST INPUT
APCS INCL U AND DERIV U INPUTS

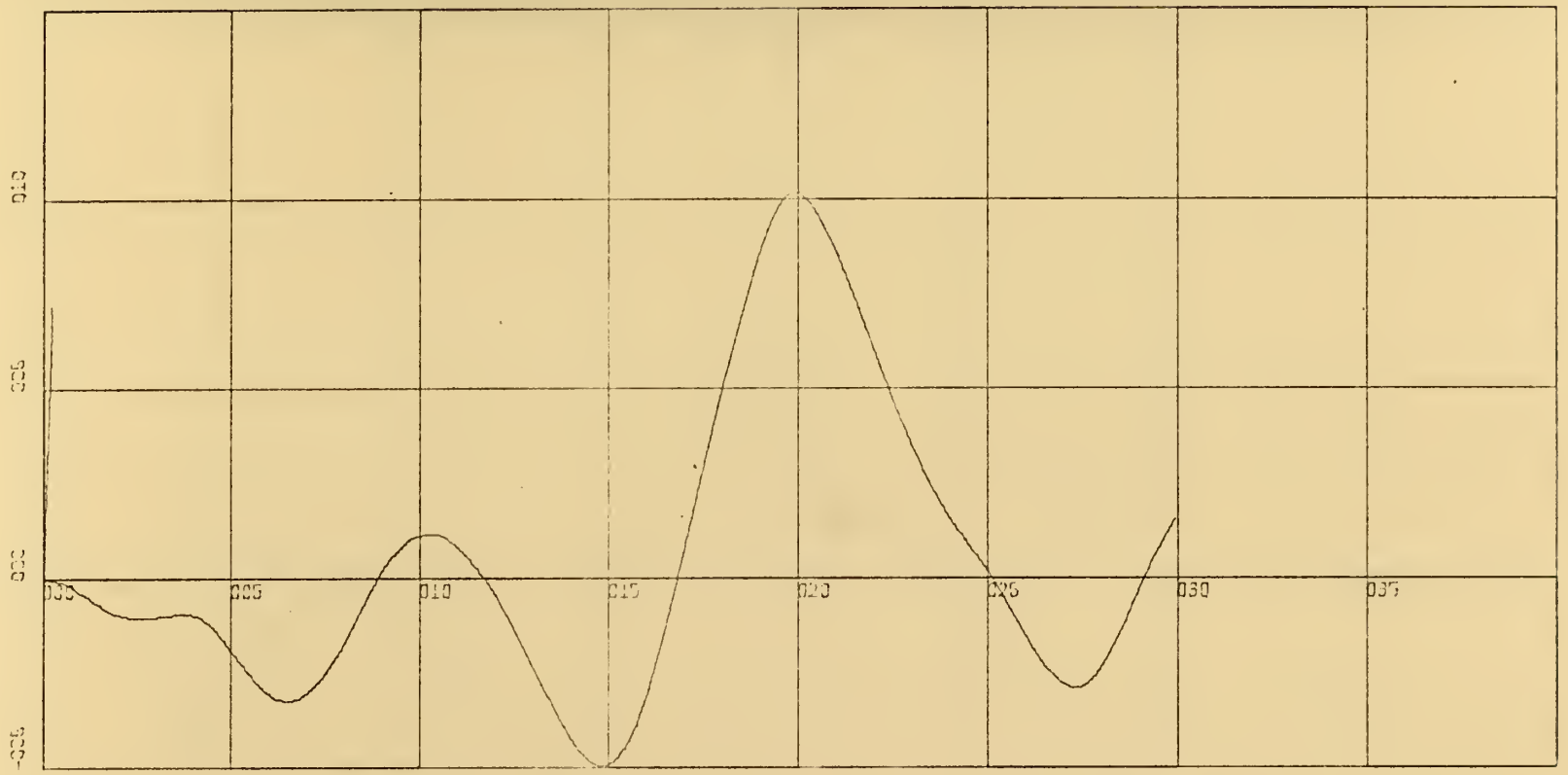

X-SCALE=5.00E+00 UNITS INCH.
Y-SCALE=5.00E+00 UNITS INCH.
ZE VS TIME U GUST INPUT
APCS INCL U AND DERIV U INPUTS

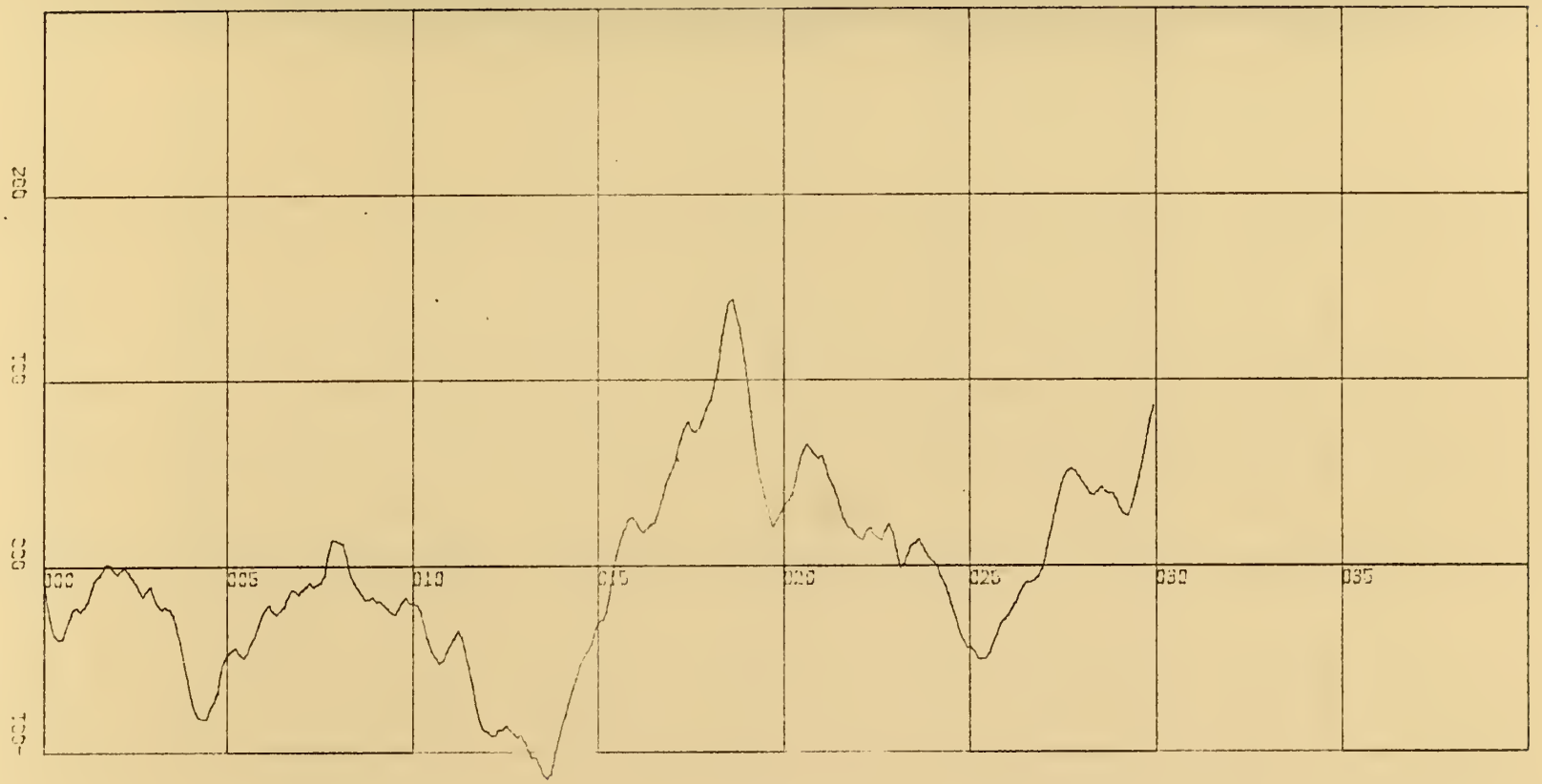

X-SCALE=5.00E+00 UNITS INCH.
Y-SCALE=1.00E+01 UNITS INCH.
UGUST VS TIME
APCS INCL U AND DERIV U INPUTS

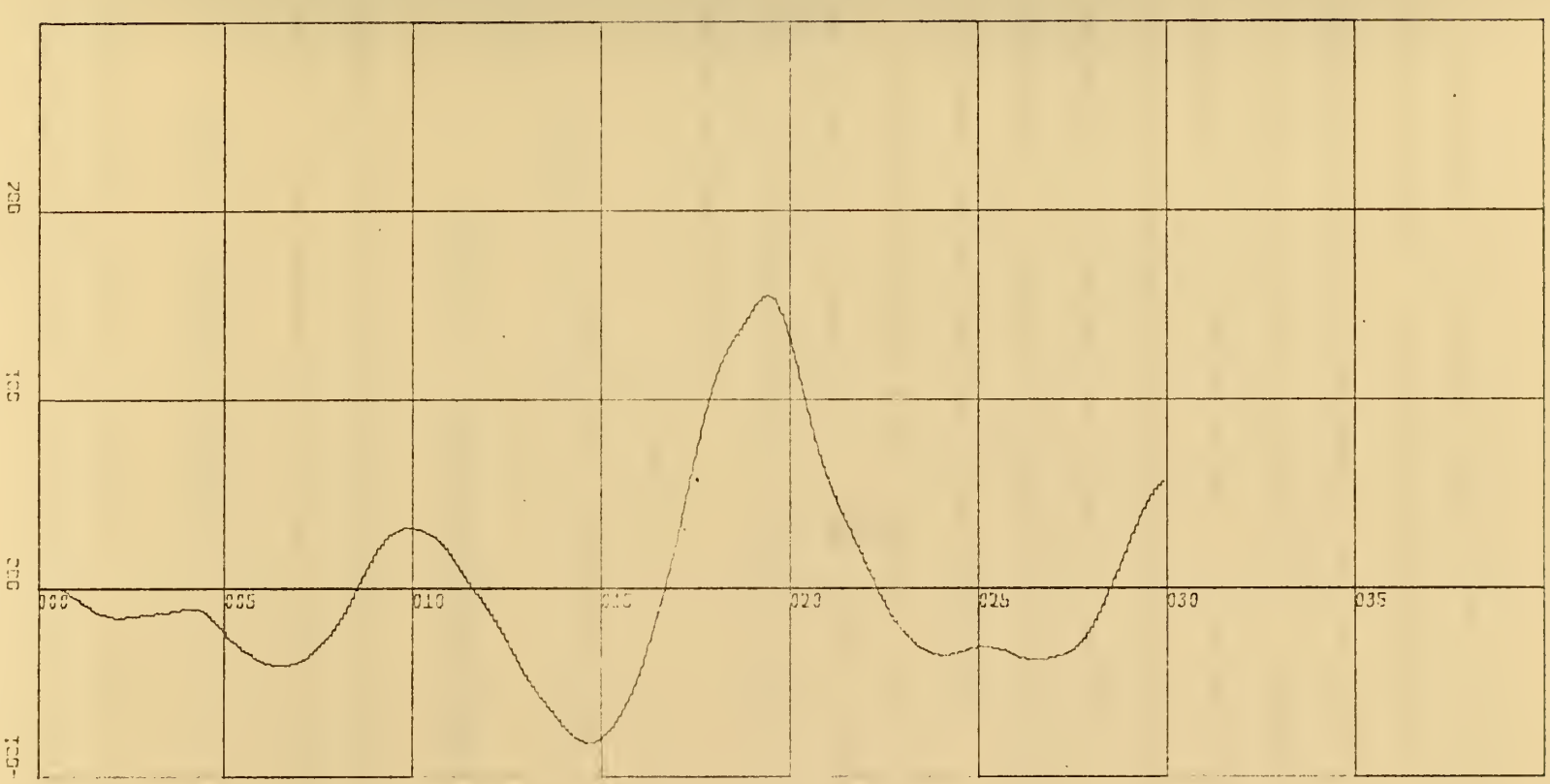

X-SCALE=5.00E+00 UNITS INCH.
Y-SCALE=1.00E+03 UNITS INCH.
THRUST VS TIME U GUST INPUT
APCS INCL U AND DERIV U INPUTS

APPENDIX B

GUST MODEL ANALYSIS

To simulate a gust input for the CSMP simulation, a random number generator was used. The CSMP function RNDGEN has a uniform probability distribution function with possible values from 0.0 to 1.0. As the desired mean of the gust input was 0.0, a constant value of 0.5 was subtracted from the RNDGEN output. The output of the random number generator was passed through a CSMP second-order filter with a break frequency of 1.0 rad/sec and a damping coefficient of 0.707 and was multiplied by a constant to achieve an RMS value of 5.0. The following is a power spectral analysis of the gust model.

Denoting the RNDGEN output signal in the frequency domain as $X(j\omega)$, the filter Fourier Transform as $H(j\omega)$, and the resultant gust signal as $Y(j\omega)$, the relationship between $X(j\omega)$ and $Y(j\omega)$ is shown in Figure B.1. The output power spectral

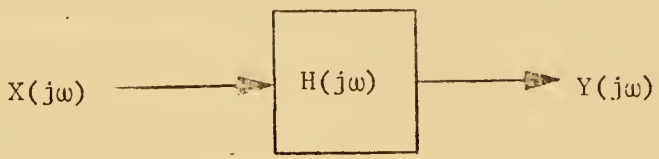

FIGURE B.1 GUST MODEL BLOCK DIAGRAM

density is equal to the input power spectral density multiplied by the absolute value squared of the filter Fourier Transform:

$$\Phi_{yy}(j\omega) = \left|H(j\omega)\right|^2 \Phi_{xx}(j\omega) \qquad (1)$$

The mean square value of the output, or average output power, can be determined by evaluating the autocorrelation function, $\varphi_{yy}(\tau)$, at $\tau = 0$:

$$\bar{y}^2 = \varphi_{yy}(0) = \frac{1}{2\pi} \int_{-\infty}^{\infty} \Phi_{yy}(j\omega)\, d\omega$$

$$= \frac{1}{2\pi} \int_{-\infty}^{\infty} |H(j\omega)|^2 \, \Phi_{xx}(j\omega) d\omega \qquad (2)$$

$\bar{y}$ is defined as the RMS value of y(t).

A typical time plot of x(t) is shown in Figure B.2.

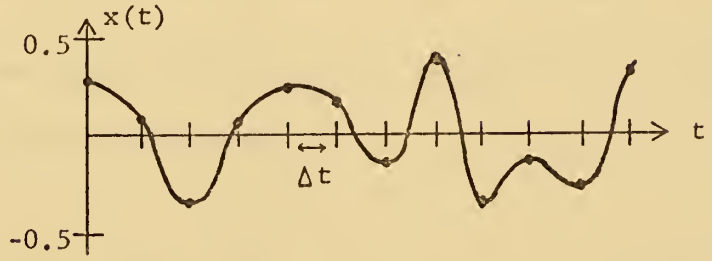

FIGURE B. 2 RNDGEN Output vs. Time

The random number generator output is a discrete value at each Δt. The resultant curve through the points represents the fourth-order Runge-Kutta approximation of the function. By approximating the curve by a series of steps, a rough approximation of the autocorrelation function, $\varphi_{xx}(\tau)$, was determined.

The autocorrelation function is defined by the equation,

$$\varphi_{xx}(\tau) = \int_{-\infty}^{\infty} x(t)\, x(t+\tau)\, dt \qquad (3)$$

For the step series function utilized to approximate the RNDGEN output, each segment, Δt in length, is uncorrelated with every other segment; that is,

$$\varphi_{xx}(\tau) = 0 \qquad |\tau| > \Delta t \qquad (4)$$

To determine $\varphi_{xx}(\tau)$ subject to the restriction of Equation (4), x(t) was depicted as in Figure B.3 [Ref. B.1]. By applying Equation (3)

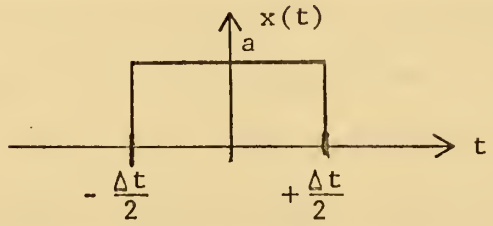

FIGURE B.3 Plot of x(t) to Determine $\varphi_{xx}(\tau)$

to Figure B.3 and requiring that $\varphi_{xx}(\tau)$ evaluated $\tau = 0$ be equal to the variance, $\varphi_{xx}(\tau)$ was determined.

$$\varphi_{xx}(\tau) = \sigma_x^2 \left(- \frac{|\tau|}{\Delta t} + 1 \right) \qquad |\tau| < \Delta t \tag{5}$$

The power spectral density can be expressed

$$\Phi_{xx}(j\omega) = \int_{-\infty}^{\infty} \varphi_{xx}(\tau) e^{-j\omega\tau} \, d\tau \tag{6}$$

By substituting Equation (5) into Equation (6) and noting that $\varphi_{xx}(\tau)$ is even function,

$$\begin{aligned} \Phi_{xx}(j\omega) &= 2\sigma_x^2 (- \frac{1}{\Delta t} \tau + 1) \cos\omega\tau \\ &= \frac{2\sigma^2}{\omega^2 \Delta t} (1 - \cos\omega\tau) \end{aligned} \tag{7}$$

By successively applying L'Hospital's Rule

$$\Phi_{xx}(0) = \sigma_x^2 \Delta t \tag{8}$$

$\Phi_{xx}(j\omega)$ is periodic with a period equal to $2\pi/\Delta t$. For a small integration step size with the filter cutoff frequency of 1.0 rad/sec, $\Phi_{xx}(j\omega)$ is essentially flat in the frequency range of interest and can be considered a constant at the zero-frequency value shown in Equation (8). For a second-order filter with a break frequency of 1.0 rad/sec, the magnitude of the transfer function, $H(j\omega)$, squared has a -40 dB/decade slope for frequencies greater than 1.0 rad/sec. Based on the flat power spectral density at low frequencies and the filter cutoff frequency, the evaluation of Equation (2) was approximated by taking $\Phi_{xx}(j\omega)$ as a constant at its zero-frequency value. The resulting integral was

$$\varphi_{yy}(0) = \sigma_x^2 \, t \cdot \frac{1}{2\pi} \int_{-\infty}^{\infty} \frac{\omega_n^2}{(j\omega)^2 + 2\zeta\omega_n(j\omega) + \omega_n^2} \, d\omega \qquad (9)$$

and was of a form tabulated in Ref. B.2. Substituting for ω_n and ζ and evaluating,

$$\varphi_{yy}(0) = 0.354\sigma_x^2 \cdot \Delta t = \bar{y}^2$$

At $\bar{y}$ = 5.0 ft/sec and Δt = 0.05 sec,

$$\sigma_x = 37.6 \text{ ft/sec} \qquad (10)$$

In actual simulation the value of σ_y was strongly dependent on the RNDGEN used in the simulation, varying from 1.7 to 3.1 with a mean of 2.4, all values falling below the predicted. RMS values of the input to the filter (the outputs of the RNDGEN's) were essentially constant at the predicted value. The underestimation of the value of σ_x required to achieve the desired value of σ_y was a direct result of the step approximation to the fourth-order integration. The reason for the large

variance in output RMS values was not determined but was suspected to be caused by the short run time. The length of each run was 30 seconds, or 3600 integration points. In the final model, σ_x was adjusted to obtain the desired value of 5.0 ft/sec for σ_y.

REFERENCES

[B.1] Blakelock, J. H., Col, USAF, Automatic Control of Aircraft and Missles, Wiley, 1965.

[B.2] Newton, G. C. Jr., Gould, L. A., and Kaiser, J. F., Analytical Design of Linear Feedback Controls, Wiley, 1957.

APPENDIX C

MULTIPLE LOOP CONTROL SYSTEM ANALYSIS

The multiple loop analysis technique described below is derived and demonstrated for a general case in Ref. C.1. The technique is a procedure for expressing specific closed loop transfer functions of a multiple loop system in terms of the elements of the open loop, feedforward and feedback matrices. The following is a two control input, three output example.

Consider the system

$$[A]\{X\} = [B]\{\delta\} + [C]\{R\}$$

$$\begin{bmatrix} a_{11}, & a_{12}, & a_{13} \\ a_{21}, & a_{22}, & a_{23} \\ a_{31}, & a_{32}, & a_{33} \end{bmatrix} \begin{Bmatrix} X_1(s) \\ X_2(s) \\ X_3(s) \end{Bmatrix} = \begin{bmatrix} b_{11}, & b_{12} \\ b_{21}, & b_{22} \\ b_{31}, & b_{32} \end{bmatrix} \begin{Bmatrix} \delta_1(s) \\ \delta_2(s) \end{Bmatrix} + \begin{bmatrix} c_{11}, & c_{12} \\ c_{21}, & c_{22} \\ c_{31}, & c_{32} \end{bmatrix} \begin{Bmatrix} R_1(s) \\ R_2(s) \end{Bmatrix} \qquad (1)$$

Matrix elements are general and may contain operators. [A] is the open loop system matrix, {X} is a vector of variables, {δ} is a vector of control variables, and {R} is a vector of external disturbances. The system will contain one feedforward and two feedback paths to drive the control variable δ_1, as depicted in Figure C.1.

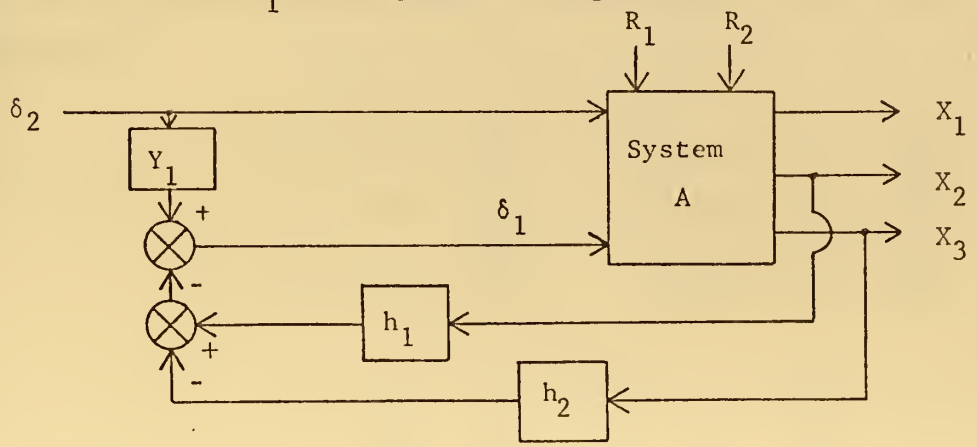

FIGURE C.1 Control System Block Diagram

The control equation is

$$\delta_1 = -h_1X_2 - h_2X_3 + Y_1\delta_2 \tag{2}$$

The (s) notation has been dropped for simplicity. Substituting Equation (2) into (1) and rearranging

$$\begin{bmatrix} a_{11}, & a_{12}+h_1b_{11}, & a_{13}+h_2b_{11} \\ a_{21}, & a_{22}+h_1b_{21}, & a_{23}+h_2b_{21} \\ a_{31}, & a_{32}+h_1b_{31}, & a_{33}+h_2b_{31} \end{bmatrix} \begin{Bmatrix} X_1 \\ X_2 \\ X_3 \end{Bmatrix}$$

$$= \begin{bmatrix} b_{12}+Y_1b_{11} \\ b_{22}+Y_1b_{21} \\ b_{32}+Y_1b_{31} \end{bmatrix} \delta_2 + \begin{bmatrix} c_{11}, & c_{12} \\ c_{21}, & c_{22} \\ c_{31}, & c_{32} \end{bmatrix} \begin{Bmatrix} R_1 \\ R_2 \end{Bmatrix} \tag{3}$$

Equation (3) is represented by the matrix notation

$$[A''] \{X\} = [B'] \{\delta_2\} + [C] \{R\}$$

where A'' denotes two loop closures and B' denotes one feedforward path. The closed loop system determinant can be expanded into a sum of four determinants

$$|A''| \equiv \Delta'' = \begin{vmatrix} a_{11}, & a_{12}, & a_{13} \\ a_{21}, & a_{22}, & a_{23} \\ a_{31}, & a_{32}, & a_{33} \end{vmatrix}_1 + \begin{vmatrix} a_{11}, & h_1b_{11}, & a_{13} \\ a_{21}, & h_1b_{21}, & a_{23} \\ a_{31}, & h_1b_{31}, & a_{33} \end{vmatrix}_2$$

$$+ \begin{vmatrix} a_{11}, & a_{12}, & h_2b_{11} \\ a_{21}, & a_{22}, & h_2b_{21} \\ a_{31}, & a_{32}, & h_2b_{31} \end{vmatrix}_3 + \begin{vmatrix} a_{11}, & h_1b_{11}, & h_2b_{11} \\ a_{21}, & h_1b_{21}, & h_2b_{21} \\ a_{31}, & h_1b_{31}, & h_2b_{31} \end{vmatrix}_4 \tag{4}$$

The determinant with a subscript of 1 is the open loop system determinant. Number 2 is the numerator of the open loop X_2/δ_1 transfer function multiplied by h_1. Number 3 is the numerator of the open loop X_3/δ_1 transfer function multiplied by h_2. Number 4 is identically equal to zero, as the second and third columns are proportional.

N_{δ}^{x} denotes the numerator of the open loop $X/\delta(s)$ transfer function. Using this notation, Equation (4) becomes

$$\Delta'' = \Delta + h_1 N_{\delta_1}^{x_2} + h_2 N_{\delta_1}^{x_3} \tag{5}$$

Equation (5) can be expanded for the general case to any order and number of closures as

$$\Delta^{n+m} = \Delta + \sum_{i=1}^{n} \sum_{j=1}^{m} h_{ij} N_{\delta_i}^{x_j} \tag{6}$$

h_{ij} represents the feedback transfer function from δ_i to x_j.

$N_{\delta_2}^{x_1}\Big]_{x_2, x_3, \delta_2 \to \delta_1}$ is defined as the closed loop numerator of the X_1/δ_2 transfer function for the above loop closures.

From Equation (3)

$$N_{\delta_2}^{x_1}\Big]_{x_2,x_3,\delta_2 \to \delta_1} = \begin{vmatrix} b_{12} + Y_1 b_{11}, & a_{12} + h_1 b_{11}, & a_{13} + h_2 b_{11} \\ b_{22} + Y_1 b_{21}, & a_{22} + h_1 b_{21}, & a_{23} + h_2 b_{21} \\ b_{32} + Y_1 b_{31}, & a_{32} + h_1 b_{31}, & a_{33} + h_2 b_{31} \end{vmatrix} \tag{7}$$

Expanding Equation (7)

$$N^{x_1}_{\delta_2}\Big]_{x_2,\, x_3,\, \delta_2 \rightarrow \delta_1} = \begin{vmatrix} b_{12}, & a_{12}, & a_{13} \\ b_{22}, & a_{22}, & a_{23} \\ b_{32}, & a_{32}, & a_{33} \end{vmatrix} + \begin{vmatrix} Y_1 b_{11}, & a_{12}, & a_{13} \\ Y_1 b_{21}, & a_{22}, & a_{23} \\ Y_1 b_{31}, & a_{32}, & a_{33} \end{vmatrix}$$

$$+ \begin{vmatrix} b_{12}, & h_1 b_{11}, & a_{13} \\ b_{22}, & h_1 b_{21}, & a_{23} \\ b_{32}, & h_1 b_{31}, & a_{33} \end{vmatrix} + \begin{vmatrix} b_{12}, & a_{12}, & h_2 b_{11} \\ b_{22}, & a_{22}, & h_2 b_{21} \\ b_{32}, & a_{32}, & h_2 b_{31} \end{vmatrix} + 0 + 0 + 0 \qquad (8)$$

Inspection of Equation (7) reveals that three determinants have dropped out. Equation (8) can be rewritten as

$$N^{x_1}_{\delta_2}\Big]_{x_2,\, x_3,\, \delta_2 \rightarrow \delta_1} = N^{x_1}_{\delta_2} + Y_1 N^{x_1}_{\delta_1} + h_1 N^{x_1 x_2}_{\delta_2 \delta_1} + h_2 N^{x_1 x_3}_{\delta_2 \delta_1} \qquad (9)$$

where

$$N^{x_1 x_2}_{\delta_2 \delta_2} \equiv \begin{vmatrix} b_{11}, & b_{12}, & a_{13} \\ b_{21}, & b_{22}, & a_{23} \\ b_{31}, & b_{32}, & a_{33} \end{vmatrix}$$

Again, Equation (9) applies in general.

In the following case the output variable is X_2, one of the feedback variables.

$$N^{x_2}_{\delta_2}\Big]_{x_2,\, x_3,\, \delta_2 \rightarrow \delta_1} = \begin{vmatrix} a_{11}, & b_{12}+Y_1 b_{11}, & a_{13}+h_2 b_{11} \\ a_{21}, & b_{22}+Y_1 b_{21}, & a_{23}+h_2 b_{21} \\ a_{31}, & b_{32}+Y_1 b_{31}, & a_{33}+h_2 b_{31} \end{vmatrix}$$

In the above notation

$$\left[N_{\delta_2}^{x_2}\right]_{x_2,\, x_3,\, \delta_2 \to \delta_1} = N_{\delta_2}^{x_2} + Y_1 N_{\delta_1}^{x_2} + h_2 N_{\delta_2\delta_1}^{x_2x_3} \tag{10}$$

In Equation (10) another crossproduct was lost. This was a special case, but the notation of Equation (9) applies, noting that the lost term would have been $h_1 N_{\delta_2\delta_1}^{x_2x_2}$. A numerator of this form makes no sense and is defined as identically zero.

The following is a numerator of a transfer function of an output variable due to an external disturbance.

$$\left[N_{r_1}^{x_1}\right]_{x_2,\, x_3,\, \delta_2 \to \delta_1} = \begin{vmatrix} c_{11}, & a_{12}+h_1 b_{11}, & a_{13}+h_2 b_{11} \\ c_{21}, & a_{22}+h_1 b_{21}, & a_{23}+h_2 b_{21} \\ c_{31}, & a_{32}+h_1 b_{31}, & a_{33}+h_2 b_{31} \end{vmatrix}$$

$$= N_{r_1}^{x_1} + h_1 N_{r_1\delta_1}^{x_1x_2} + h_2 N_{r_1\delta_1}^{x_1x_3} \tag{11}$$

Equation (11) is similar to Equation (9), but the feedforward term is missing. The notation of equation (11) applies to any external input for which there is no feedforward term, either for another control variable or for an actual external disturbance, as illustrated.

It should be noted that $N_{\delta_1\delta_2}^{x_2x_3}$ and $N_{\delta_2\delta_1}^{x_3x_2}$ denote the same determinant; i.e., rows are not interchanged. The latter notation would arise if $\left[N_{\delta_2}^{x_3}\right]_{x_2,\, x_3,\, \delta_2 \to \delta_1}$ were formed.

REFERENCE

[C.1] Air Force Flight Dynamics Laboratory Report TDR-62-1014, Analysis of Multiloop Vehicular Control Systems, by D. T. McRuer, I. L. Ashkenas, and H. R. Pass, March 1964.

INITIAL DISTRIBUTION LIST

		No. Copies
1.	Defense Documentation Center Cameron Station Alexandria, Virginia 22314	2
2.	Library, Code 0212 Naval Postgraduate School Monterey, California 93940	2
3.	Chairman, Department of Aeronautics Naval Postgraduate School Monterey, California 93940	1
4.	Professor R. A. Hess, Code 57He Department of Aeronautics Naval Postgraduate School Monterey, California 93940	1
5.	LT D. H. Finney, USN 451 Dela Vina Avenue, Apt. 412 Monterey, California 93940	1
6.	Commander Naval Air Systems Command (PMA-235) Navy Department Washington, D. C. 20360	1
7.	Professor G. J. Thaler, Code 52Tr Department of Electrical Engineering Naval Postgraduate School Monterey, California 93940	1

DOCUMENT CONTROL DATA - R & D

(Security classification of title, body of abstract and indexing annotation must be entered when the overall report is classified)

1. ORIGINATING ACTIVITY (Corporate author)
Naval Postgraduate School
Monterey, California 93940

2a. REPORT SECURITY CLASSIFICATION
Unclassified

2b. GROUP

3. REPORT TITLE

A REVISED DESIGN CONCEPT FOR THE A-7E APPROACH POWER COMPENSATOR SYSTEM

4. DESCRIPTIVE NOTES (Type of report and, inclusive dates)
Master's Thesis; March 1973

5. AUTHOR(S) (First name, middle initial, last name)
DAVID H. FINNEY

6. REPORT DATE
March 1973

7a. TOTAL NO. OF PAGES
91

7b. NO. OF REFS
12

8a. CONTRACT OR GRANT NO.

b. PROJECT NO.

c.

d.

9a. ORIGINATOR'S REPORT NUMBER(S)

9b. OTHER REPORT NO(S) (Any other numbers that may be assigned this report)

10. DISTRIBUTION STATEMENT

Approved for public release; distribution unlimited.

11. SUPPLEMENTARY NOTES

12. SPONSORING MILITARY ACTIVITY
Naval Postgraduate School
Monterey, California 93940

13. ABSTRACT

The present concept of automatic throttle control, as employed in Navy carrier-based aircraft, was investigated. The aircraft chosen for study was the A-7E. The powerplant was the TF41-A-2, a turbofan engine with a relatively slow throttle response in the approach power range.

The effects of additional inputs to the approach power compensator were evaluated. It was shown that a considerable increase in performance could be achieved through the incorporation of longitudinal feedback. In addition, the limitations imposed on performance by large engine lags were found to be much less severe for systems with longitudinal feedback. The modifications suggested require a redesign of the approach power compensator system currently in use by the Navy.

14. KEY WORDS	LINK A		LINK B		LINK C	
	ROLE	WT	ROLE	WT	ROLE	WT
APPROACH POWER COMPENSATOR SYSTEM						
AUTOMATIC THROTTLE CONTROL						
AUTOMATIC POWER CONTROL						
AIRSPEED CONTROL						
AUTOMATIC CARRIER LANDING						
A-7E AIRCRAFT						

142025
Thesis
F4463 Finney
c.1 A revised design concept for the A-7E approach power compensator system.

142025
Thesis
F4463 Finney
c.1 A revised design concept for the A-7E approach power compensator system.

thesF4463
A revised design concept for the A-7E ap
3 2768 002 00172 9
DUDLEY KNOX LIBRARY